GUIDANCE AND CONTROL OF SATURN LAUNCH VEHICLES

by

WALTER HAEUSSERMANN
National Aeronautics and Space Administration
Marshall Space Flight Center
Huntsville, Alabama

AIAA Paper
No. 65-304

AIAA Second Annual Meeting
SAN FRANCISCO, CALIFORNIA / JULY 26-29, 1965

GUIDANCE AND CONTROL OF SATURN LAUNCH VEHICLES

by

WALTER HAEUSSERMANN
Director of the Astrionics Laboratory
George C. Marshall Space Flight Center
National Aeronautics and Space Administration

ABSTRACT

The navigation, guidance, and control modes and problems of the Saturn launch vehicles are given as the requirements for the guidance and control methods. Two path adaptive guidance modes, featuring flight path optimization, in the form of a polynomial mode and an iterative mode are given in their computation form and compared with respect to mission flexibility, implementation requirements, and performance. Attitude control during the propelled flight phases requires consideration of various bending and sloshing modes; stability of the control system is obtained by phase stabilization of the low frequencies and by attenuation of the higher frequencies. Typical shaping networks and their transfer functions are given. The attitude control system during coasting periods is briefly described. The functional behavior and characteristic data of the main guidance and control hardware such as the inertial sensors, stabilized platform, digital computer, data adapter, control computer, and actuation system are described. Reliability requirements are emphasized. The principle of redundancy is extensively used to obtain highest reliability for long operating times. Data and results from recent Saturn I flights summarize the performance of the guidance schemes.

1. NAVIGATION, GUIDANCE, AND CONTROL MODES OF THE SATURN LAUNCH VEHICLE

The mission of the Saturn V launch vehicle is to inject the Apollo spacecraft into a translunar trajectory and to provide navigation, guidance, and control functions until separation from the spacecraft is accomplished. To perform this mission, the Saturn V is equipped with one navigation, guidance, and control system, located in the Instrument Unit (IU) on top of the S-IVB stage, and with various propulsion means (rocket motors and nozzles). Locations and some characteristic data of this equipment are shown in Figure 1-1.

Note: A conversion table of SI units to English equivalents is shown on page 70.

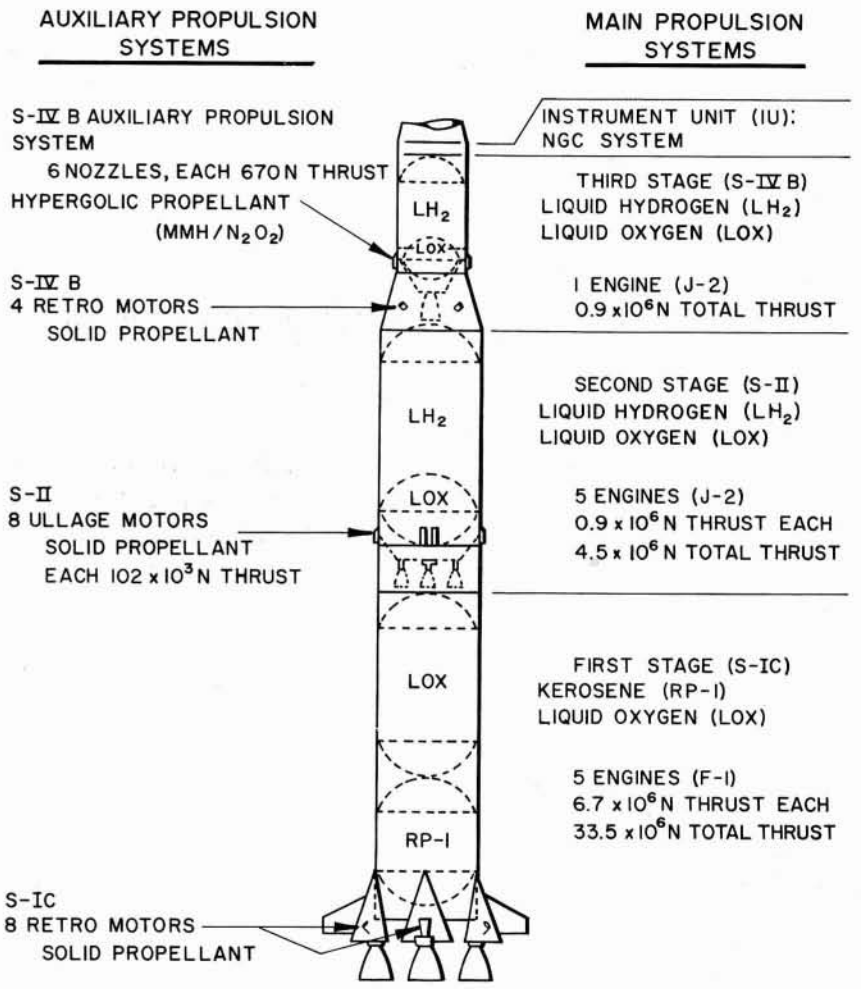

Figure 1-1. Saturn V Launch Vehicle.

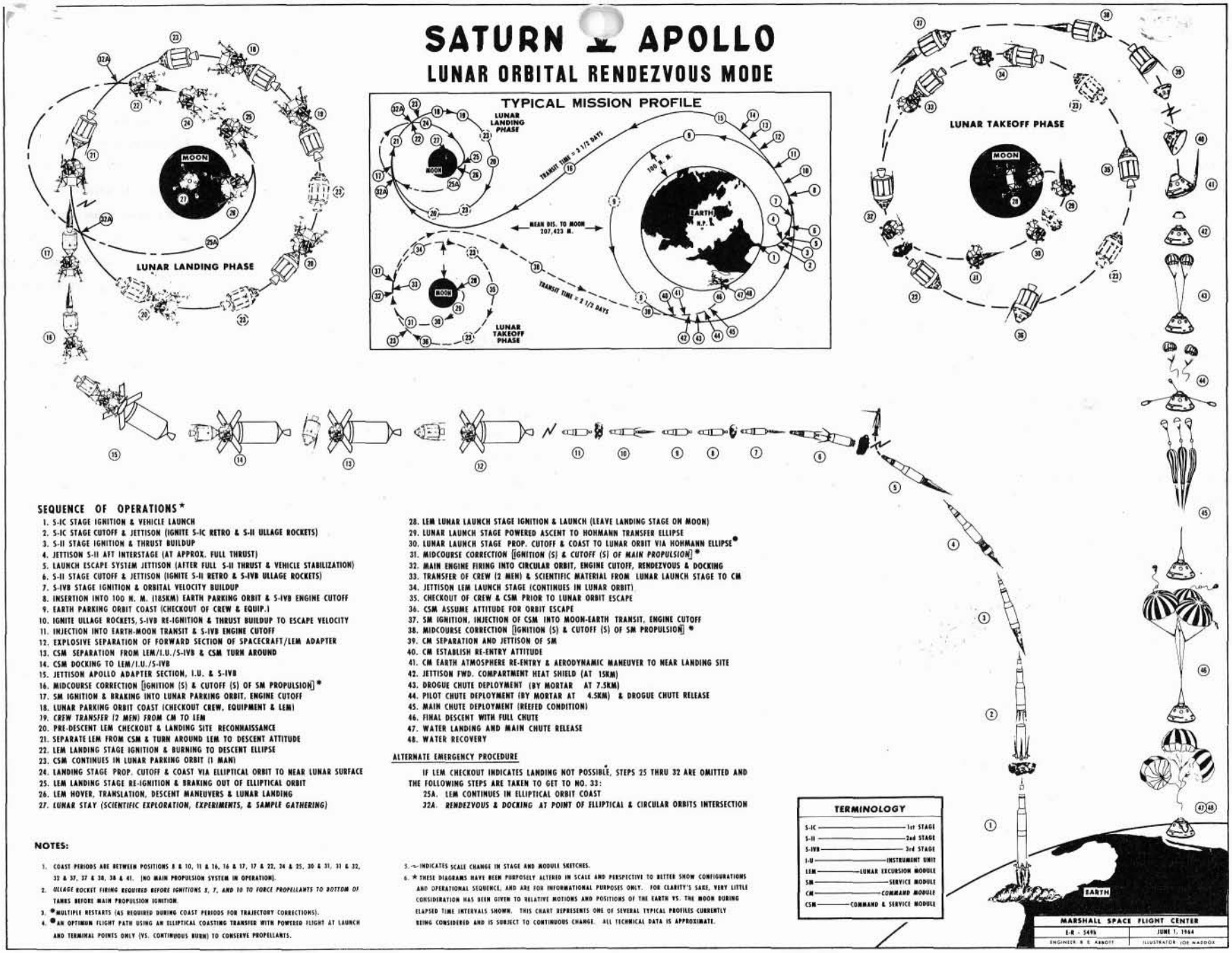

Figure 1-2 Saturn V Apollo Lunar Orbital Rendezvous Mode.

The Saturn navigation, guidance, and control system controls all stages of the launch vehicle. It is an inertial system that can be updated by radio transmission from ground stations. The main components of the inertial navigation, guidance, and control system are the stabilized platform, the digital guidance computer and data adapter, and the control computer. The platform serves as an inertial reference frame for attitude control and acceleration measurements. The digital guidance computer performs navigation and guidance computations and generates control commands, including discrete sequencing signals (engine cutoff, stage separation, etc.). During flight, information can be inserted into the guidance computer from ground stations through a radio command link. The control computer accepts signals from the guidance computer, stabilized platform, rate gyros, and control accelerometers to generate the proper attitude control commands.

The important hardware components of the navigation, guidance, and control system are described in Chapter 4. The following discussion is a brief survey of the navigation, guidance, and control modes of the Saturn V flight phases. The sequence of flight events is illustrated in Figure 1-2. More details and basic information are given in Chapters 2 and 3.

First Stage Flight

The five engines of the first stage (S-IC) generate a total thrust of 34×10^6N. Attitude control and guidance maneuvers are executed by swiveling the four outer engines.

On the launch pad, the vehicle always has a roll orientation fixed to the launching site. Thus, after vertical takeoff from the launch pad, it must perform a programed roll maneuver to align itself to the desired flight azimuth. About the same time, the tilt program is initiated by the guidance system, which sends a pitch command to the control system. The roll and pitch commands are stored in the guidance computer and are functions of time only. The first stage flight uses a standard tilt program (open loop guidance) instead of closed loop guidance. Beginning with liftoff, position and velocity data are computed from accelerometer measurements.

The vehicle traverses the dense portion of the atmosphere during the first stage flight only. Structural loads from aerodynamic forces are kept within a tolerable range by controlling the vehicle to achieve a minimum angle of attack. For the same reason, guidance corrections are not introduced. Aerodynamic pressure reaches a maximum at approximately 12 km altitude (77th second of flight time).

The control system keeps the angle of attack below the safety limit of 10 degrees by using lateral accelerometer control. Stable control conditions are achieved by proper location of angular rate sensors and application of phase-shifting networks. Propellant sloshing is reduced by baffles in the propellant tank rather than by active control.

Second Stage Flight

The five engines of the second stage generate a total thrust of 4.5×10^6N. As in the first stage, the four outer engines can be swiveled for attitude control and guidance maneuvers.

Beginning with the ignition of the second stage, a path adaptive guidance scheme is used at orbit insertion to guide the vehicle on a "minimum propellant" trajectory to the aim conditions, which are stored in the guidance computer. A detailed discussion of two guidance schemes that have been developed is given in Chapter 2. Since the second and third stage flight is practically outside the atmosphere, where atmospheric disturbances and forces no longer exist, the function of the control system is reduced to controlling the thrust direction as commanded by the guidance system. Control signals from the inertial platform and rate gyros (in the Instrument Unit) are used.

Third Stage Flight

Main propulsion of the third stage (S-IVB) is provided by a single $.9 \times 10^6$N thrust engine, similar to one of the second stage engines, which can be swiveled for thrust direction control. Since roll control cannot be obtained with a single engine, it is achieved by an auxiliary propulsion system, which is also used during coasting periods. This system uses six control nozzles (two for pitch, four for yaw and roll) mounted body-fixed on the outside of the stage structure. The same guidance and control scheme and system that serve second stage engine actuation are used for the third stage actuators.

The engine is ignited the first time after separation of the second stage. At this time, the vehicle has reached approximately orbital altitude and the first burn of the S-IVB provides the required orbital speed. The guidance system commands engine cutoff when the vehicle has gained the precalculated orbital velocity.

Acceleration, velocity, and aerodynamic pressure for a typical Saturn V powered flight trajectory into earth orbit are shown in Figure 1-3. The step in the $\frac{F}{m}$ curve around 420 seconds is

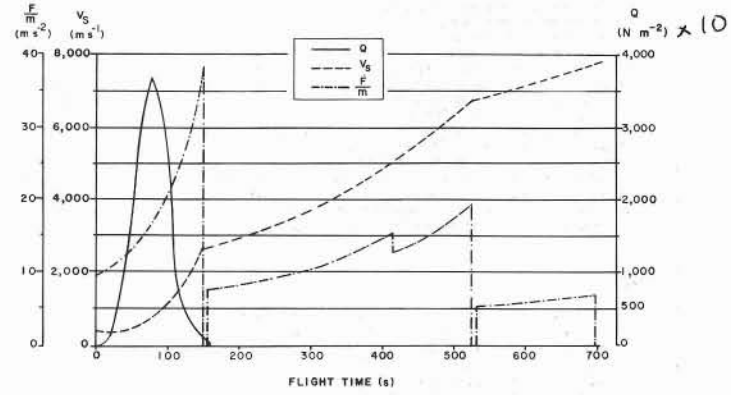

Figure 1-3. Acceleration, Velocity, and Aerodynamic Pressure for a Typical Saturn V Trajectory.

caused by a change of the propellant mixture ratio to increase the specific impulse which, however, reduces the thrust and therefore cannot be applied earlier.

During orbital flight, tracking from ground stations of the Manned Space Flight Network is used in addition to onboard navigation to determine the orbit of the vehicle. If required, position and velocity information in the launch vehicle guidance computer can be updated from tracking data by transmission from ground stations.

Translunar Injection

For injection out of orbit into a translunar trajectory, the S-IVB engine is ignited a second time. Re-ignition times for the S-IVB are computed in the vehicle's guidance computer for each orbit. The launch vehicle navigation, guidance, and control system guides the space vehicle during translunar injection. However, the Apollo spacecraft navigation and guidance system can be used for injection in case of a malfunction in the Saturn navigation and guidance system. Control of the space vehicle is accomplished in the same manner as during the first burn of the S-IVB stage.

Engine cutoff is commanded by the guidance system when the required injection conditions have been achieved. The space vehicle is now on a predetermined "free-return" trajectory to the moon.

Transposition Maneuver and Separation

Within a period of approximately one hour after S-IVB engine cutoff, the transposition maneuver is executed. In this maneuver, the S-IVB/IU provides attitude stabilization for the Lunar Excursion Module, while the Command and Service Modules are separated from the Lunar Excursion Module, turned around, and docked with the Lunar Excursion Module. After completion of this maneuver, the S-IVB/IU is disengaged from the Apollo spacecraft. Thus the launch vehicle mission is completed; its maximum total mission time is 6 1/2 hours.

2. SATURN LAUNCH VEHICLE PATH ADAPTIVE GUIDANCE

2.1 Introduction to Launch Vehicle Guidance Problems [1]

The problem of directing a space vehicle to accomplish a given mission is customarily discussed in terms of three separate functions: navigation, guidance, and control. Navigation is the determination of the vehicle's state (e.g., position and velocity) from onboard measurements; guidance is the computation of flight maneuvers required to achieve the mission goal; control is the execution of the maneuvers called for by guidance.

The guidance scheme is represented by a set of equations programed into the guidance computer. Input to these guidance equations is the navigation information defining the instantaneous state of the vehicle. The required orientation of the thrust vector and the time of engine cutoff and re-ignition are computed according to the guidance scheme.

Usually, many constraints apply to vehicle trajectories and flight maneuvers. The initial

conditions of a trajectory are given by the location of the launch site on earth or the time of launch from a parking orbit. To achieve the mission objective, the vehicle must meet certain conditions at the ends of powered flight phases. A variety of such end conditions, depending on the particular mission, exists for space flight trajectories. For instance, the position and velocity vector at the time of engine cutoff may be specified. Time may also be included; i.e., the vehicle must meet the specified end conditions at a given time. In the Apollo mission, the end conditions for the Saturn V launch vehicle trajectory are defined at insertion into earth orbit and at injection into translunar trajectory. Both end conditions are functions of time because the launch point and the target (i.e., the moon) move through space. The orientation of the orbital plane is defined by the center of the earth, the launch point, and the position of the moon at the desired time of arrival. To achieve this plane, the launch azimuth must be a function of launch time. Figure 2.1-1 shows the variation of corresponding parameters with time of launch for a typical situation. The specified end conditions at orbit insertion can be expressed as direction and magnitude of the velocity vector and altitude at the moment of engine cutoff. The end conditions can be considered launch time independent if the velocity vector orientation is varied by the launch azimuth.

The guidance commands required to bring the vehicle from its initial or instantaneous state to the desired end conditions must be compatible with the constraints imposed by control and structural limitations. Therefore the Saturn launch vehicle does not use closed loop guidance during the first stage propulsion phase. Consequently, comparatively large deviations from a non-perturbed optimum trajectory can occur and a constraint to this trajectory would result in inefficient fuel utilization. For this reason, the Saturn launch vehicle uses a path adaptive guidance scheme which derives a new adapted optimum trajectory from the instantaneous state of the vehicle; thus the onboard digital computer system computes the flight corrections and the required end conditions continuously with a rate of approximately once per second during the flight.

Several path adaptive guidance schemes have been developed for the Saturn launch vehicle. The polynomial guidance mode (PGM) and the iterative guidance mode (IGM), which are described in the following sections, have been successfully flown in Saturn I vehicles.

2.2 Polynomial Guidance Scheme [2]

The polynomial path adaptive guidance scheme [3,4] was formulated to correct large variations in vehicle performance with good propellant economy and accuracy. The scheme provides guidance commands that cause a minimum propellant trajectory connecting the instantaneous position of the vehicle with the desired terminal point. The trajectory is generated from the instantaneous state variables and parameter values that are characteristic of the vehicle performance. For a flight path outside the atmosphere, this performance is mainly a function of the acceleration

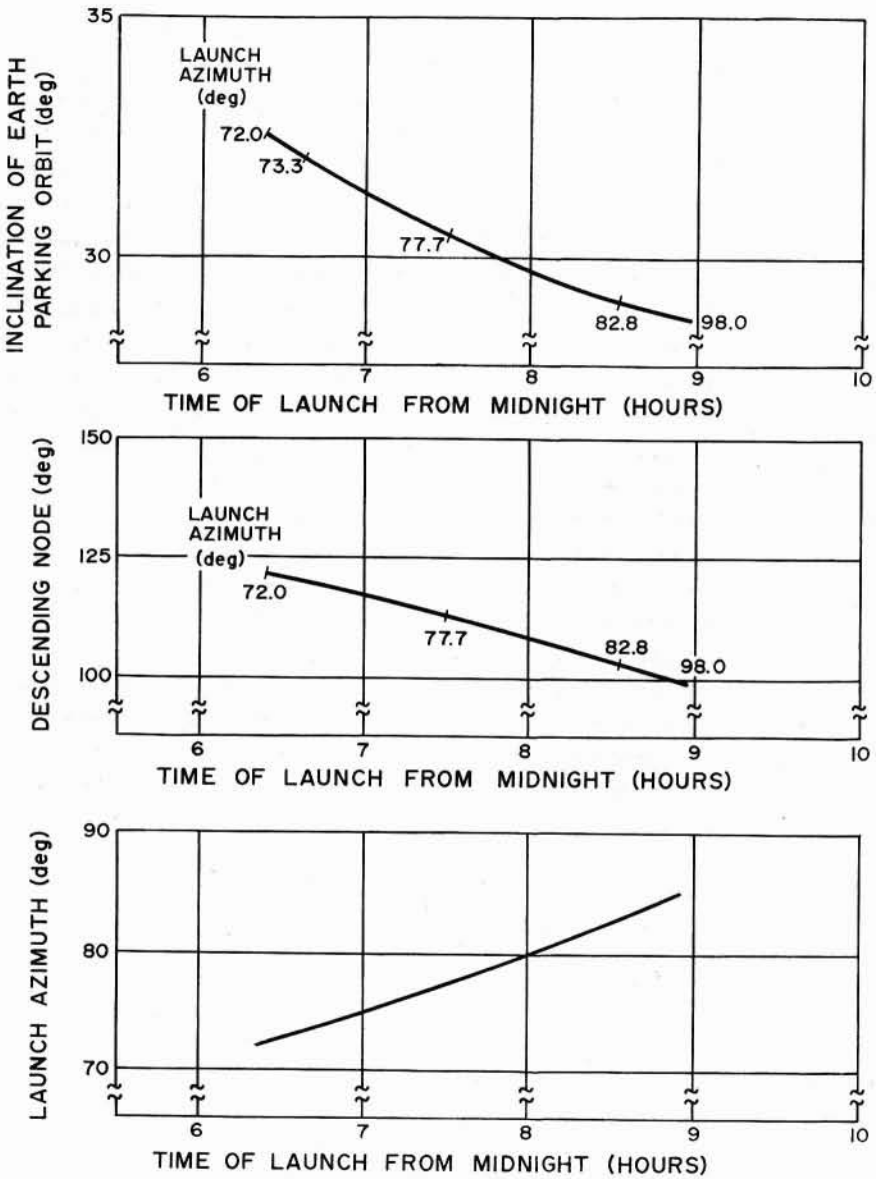

Figure 2.1-1. Variation of Corresponding Parameters with Time of Launch for a Typical Situation.

$\frac{F}{m}$ and the average specific impulse of the engines I_{sp}. Thus the optimum trajectory, starting at a point which is defined by the position vector $\bar{R}$ and moving with the velocity $\dot{\bar{R}}$, is determined by the initial conditions $\bar{R}$, $\dot{\bar{R}}$, $\frac{F}{m}$, I_{sp}, t and the cutoff or end conditions $\bar{R}_c$, $\dot{\bar{R}}_c$, t_c. Associated with the flight path are functions for the Eulerian angles χ_p and χ_y, which define the thrust direction along the minimum propellant trajectory.

Under perturbations, the instantaneous points, from which minimum propellant trajectories can start, fill a certain volume in space which therefore is also defined by the sum of all the possible minimum propellant flight paths. To each point in this spatial volume belong thrust directions, which are a function of the instantaneous state variables and performance parameters $\bar{R}$, $\dot{\bar{R}}$, $\frac{F}{m}$, I_{sp}, t, and the trajectory end conditions, which may be constant data or a function of time. Thus the guidance equations may be written in functional form for the thrust direction as

$$\chi_p = f_1[\bar{R}, \dot{\bar{R}}, \frac{F}{m}, I_{sp}, t]$$

$$\chi_y = f_2[\bar{R}, \dot{\bar{R}}, \frac{F}{m}, I_{sp}, t] \qquad (2.2\text{-}1)$$

and for the flight time to cutoff as

$$t_f = f_3[\bar{R}, \dot{\bar{R}}, \frac{F}{m}, I_{sp}, t]. \qquad (2.2\text{-}2)$$

The initial values of the state variables and performance parameters are updated continuously during flight. If these functions can be found and solved during flight, the guidance commands will yield the minimum propellant trajectory.

One technique of the path adaptive guidance scheme is to express the functions for χ_p and χ_y in polynomial form. Experience has shown that the specific impulse may be omitted with negligible loss in performance. Furthermore, the equation for the remaining time of propelled flight is not needed as cutoff information for most applications. Instead, cutoff can often be initiated when the vehicle velocity reaches a desired preset value. The path adaptive guidance equations then take the form (for definition of coordinates, see Figure 2.2-1)

$$\chi_p = A_1 + A_2X + A_3Y + A_4Z + A_5\dot{X} + A_6\dot{Y} + A_7\dot{Z} + A_8(\frac{F}{m}) + A_9t + \text{higher order terms.}$$

$$\chi_y = B_1 + B_2X + B_3Y + B_4Z + B_5\dot{X} + B_6\dot{Y} + B_7\dot{Z} + B_8(\frac{F}{m}) + B_9t + \text{higher order terms.} \qquad (2.2\text{-}3)$$

The coefficients of the polynomials are evaluated by perturbation techniques and curve fitting procedures. A set of expected perturbations such as thrust deviations, weight uncertainties, one engine failure in the multiengine first or second stage, and uncertainties in engine specific impulse is selected for each stage of the vehicle (Table 2.2-1). A minimum propellant trajectory is calculated with the techniques of the calculus of variations for each perturbation and for all combinations

Table 2.2-1. Perturbations Used in the SA-7 Path Adaptive Guidance Mode Studies

STANDARD	
Propellant Variation	-5000 kg
Propellant Variation	-2500 kg
Propellant Variation	±1000 kg
Propellant Variation	±500 kg
Structure Variation	+5000 kg
Structure Variation	+2500 kg
Headwind	3σ
Tailwind	3σ
Right Crosswind	3σ
Engine No. 3 Out	100 s
Thrust and Mass Flow Variation	±1%
I_{sp} Variation	±1%

of perturbations for the different stages. For a two stage vehicle, approximately 100 trajectories are required.

The method of least squares is applied to fit the guidance command polynomials to these trajectories. The polynomials are determined here from the minimum or zero condition of the expression

$$\sum_{i=1}^{n} [\chi_{pi} - (A_1 + A_2X + A_3Y + A_4Z + A_5\dot{X} + A_6\dot{Y} + A_7\dot{Z} + A_8(\frac{F}{m}) + A_9t + \ldots)]^2 = 0 \qquad (2.2\text{-}4)$$

where n is the total number of points. Again, as mentioned in the preceding paragraphs, the least squares criterion does not insure a good curve fit and the polynomials must be verified on simulated flights.

The number of terms, and the specific terms required, in the polynomial must be determined from trial. Numerous trajectory studies and some flight testing have shown that about 35 terms are required for each of the command equations 2.2-4 to insure good accuracy and propellant economy.

The principal disadvantages of the scheme are the large number of trajectories that must be generated to produce the polynomials and the necessity for generating new polynomials for even minor changes in mission and vehicle characteristics. Moreover, each new polynomial poses a time consuming task in reprograming the digital flight computer.

Engine cutoff may be initiated by the equation

$$V_c - V_m = 0 \qquad (2.2\text{-}5)$$

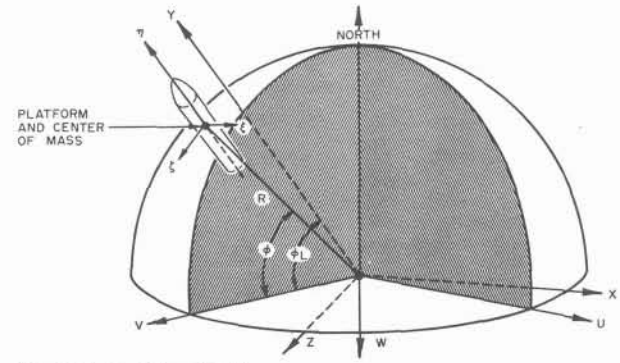

ϕ_L Geodetic latitude of launch site.

(ξ, η, ζ) Inertial coordinate system established by the orientation of the accelerometers on the stabilized platform. This is the system in which measurements are made. This system is parallel to the system (X,Y,Z) at launch.

(X,Y,Z) Space-fixed coordinate system for guidance computations. The origin is at the center of the earth, the Y axis is parallel to the launch vertical, the X and Y axes define the flight plane, and the Z axis is in the right-handed relation to X and Y.

(U,V,W) Space-fixed coordinate system. The origin is at the center of the earth, the W axis is directed toward the south pole, and the U and V axes are contained in the equatorial plane. The V-W plane contains the launch point.

Figure 2.2-1. Guidance Coordinate Systems.

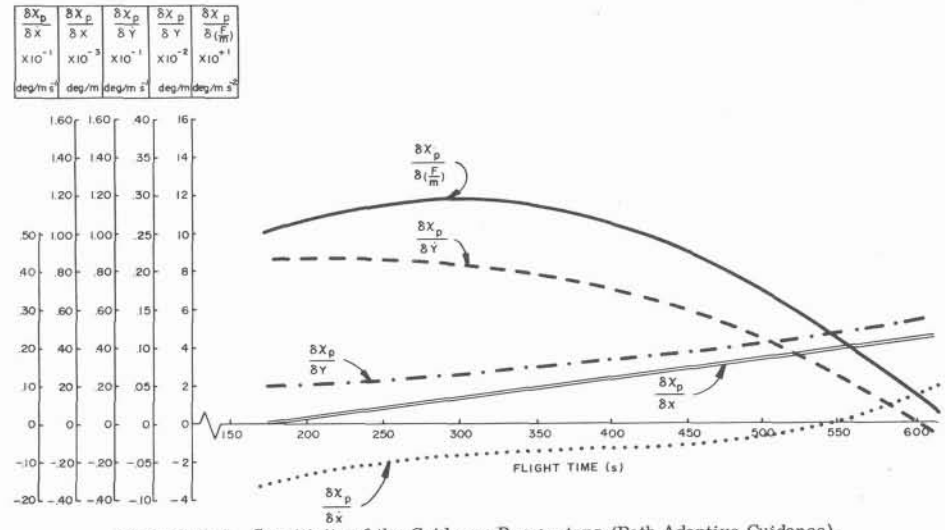

Figure 2.2-2. Sensitivity of the Guidance Parameters (Path Adaptive Guidance).

where V_c and V_m are the magnitudes of the preset cutoff velocity and the measured velocity, respectively.

A block diagram showing the guidance equation for a single guided stage flying in a plane is shown in Table 2.2-2. The sensitivity of some representative guidance command parameters χ_p to variations in the state and performance variables is shown in Figure 2.2-2.

Table 2.2-2. Path Adaptive Pitch Plane Guidance.

PRESETTING

$A_1, A_2, A_3, A_4, A_5, A_6, A_7, A_8$

$A_9, A_{10}, A_{11}, A_{12}, A_{13}, A_{14}, A_{15}, A_{16}$

$A_{17}, A_{18}, A_{19}, A_{20}, A_{21}, A_{22}, A_{23}, A_{24}$

$A_{25}, A_{26}, A_{27}, A_{28}, A_{29}, A_{30}, A_{31}, A_{32}, A_{33}$

V_c

MEASURED QUANTITIES

$\dot{\xi}, \dot{\eta}, \dot{\zeta}, t$

(For definition of coordinates, see Figure 2.2-1)

NAVIGATION AND AUXILIARY COMPUTATION

$X, Y, Z, \dot{X}, \dot{Y}, \dot{Z}$

$\ddot{X}_g, \ddot{Y}_g, \ddot{Z}_g$ (components of gravitational acceleration)

$\left(\frac{F}{m}\right)$ vehicle acceleration

TYPICAL PITCH COMMAND EQUATION

$$\chi_p = A_1 + A_2X + A_3Y + A_4\dot{X} + A_5\dot{Y} + A_6\frac{F}{m} + A_7t + A_8XY + A_9\dot{X}Y$$
$$+ A_{10}\dot{X}^2 + A_{11}X\dot{Y} + A_{12}Y\dot{Y} + A_{13}Y\frac{F}{m} + A_{14}\left(\frac{F}{m}\right)^2 + A_{15}\dot{X}t + A_{16}t^2$$
$$+ A_{17}X^3 + A_{18}XY^2 + A_{19}Y\dot{X}^2 + A_{20}Y^2\frac{F}{m} + A_{21}Y\dot{X}\frac{F}{m} + A_{22}X\dot{Y}\frac{F}{m}$$
$$+ A_{23}\dot{X}\dot{Y}\frac{F}{m} + A_{24}\dot{Y}\left(\frac{F}{m}\right)^2 + A_{25}X^2t + A_{26}Y^2t + A_{27}Y\dot{X}t + A_{28}\dot{X}\dot{Y}t$$
$$+ A_{29}\dot{X}\frac{F}{m}t + A_{30}\left(\frac{F}{m}\right)^2t + A_{31}Xt^2 + A_{32}\dot{X}t^2 + A_{33}\dot{Y}t^2$$

CUTOFF COMPUTATION

$V_m = \sqrt{\dot{X}^2 + \dot{Y}^2}$

$V_c - V_m = 0$

PITCH CONTROL SIGNAL

CUTOFF SIGNAL

2.3 Iterative Guidance Scheme [5,6,7,8,22,23]

The iterative guidance scheme was developed to meet the mission flexibility requirement of large space vehicles with minimum propellant consumption. The same optimizing techniques of the calculus of variations are used that were applied in the path adaptive guidance scheme. Experience with hundreds of minimum propellant trajectories for various orbital injection missions has demonstrated that the optimum thrust direction relative to the local vertical is very nearly a linear function of time during vacuum flight. Moreover, the size of the angle between the optimum thrust direction and the local horizon is never very large, as is shown in Figure 2.3-1, for an orbital mission. These observations show a remarkable agreement with the mathematical results obtained from the calculus of variations when a flat earth model having a constant gravitational field is used and position and velocity constraints are imposed at cutoff. A closed solution can be obtained with this mathematical model and yields an explicit equation for the optimum thrust direction [9]. This equation has the form

$$\chi_p = \arctan(A + Bt) \qquad (2.3\text{-}1)$$

where χ_p is the optimum thrust direction for minimum propellant consumption. Constants A and B are determined by the specified cutoff velocity and position, the initial values of the state variables, the vehicle thrust acceleration, and the engine specific impulse. The comparison of this equation with the results of trajectory studies suggests the use of the approximation

$$\chi_p = A + Bt. \qquad (2.3\text{-}2)$$

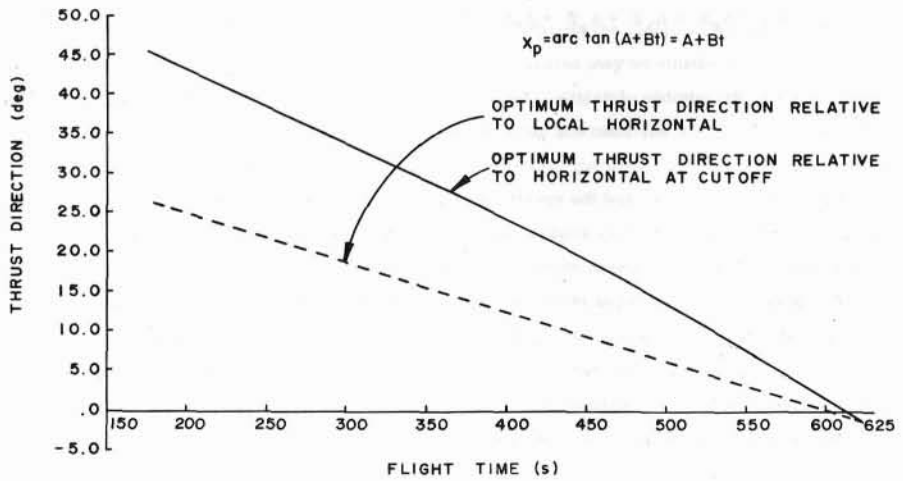

Figure 2.3-1. Optimum Thrust Angle Profile.

A guidance coordinate system (X_V, Y_V, Z_V) (Fig. 2.3-2) is established with the origin at the center of the earth and with the Y_V axis lying along the vertical which intersects the calculated cutoff position of the vehicle. Simplified equations of motions are derived to approximate the motion over an oblate earth with a realistic gravitational field. These equations of motion are solved during flight to determine the instantaneous range angle to cutoff, the time-to-go to cutoff, and the gravitational effects occurring over the remaining flight time. This information is used to compute values for A and B continuously during flight. In practice, only the value of A need be calculated when computation rates on the order of one or more per second are used, except during the last few seconds before cutoff when both A and B are computed and held constant over the remaining flight

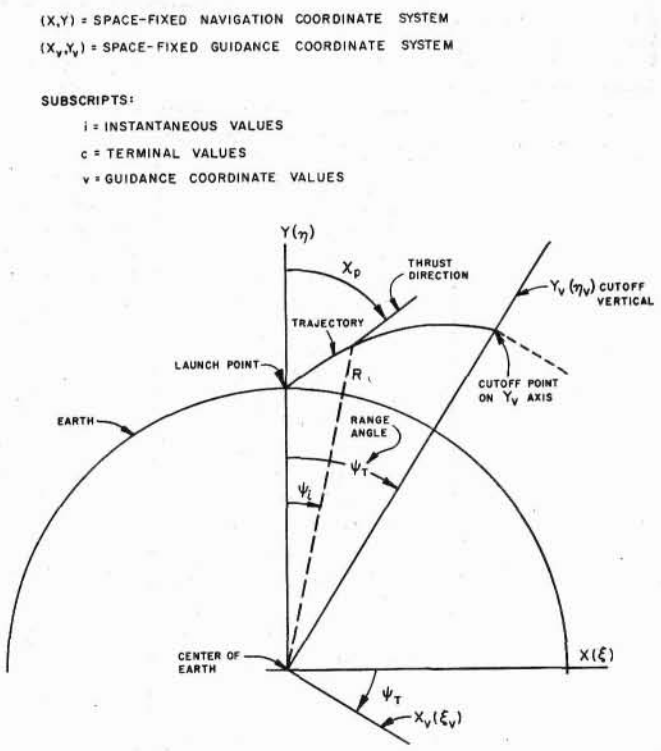

Figure 2.3-2. Coordinate System of the Iterative Guidance Scheme.

time. This is necessary because the equation gives an indeterminate command angle at the cutoff point. A representative set of equations for pitch plane guidance of a single stage is shown in Tables 2.3-1 and 2.3-2[10]. A simple velocity presetting or energy equation may be used to initiate engine cutoff.

The sensitivity of the guidance parameter to position, velocity, and thrust acceleration is shown in Figure 2.3-3.

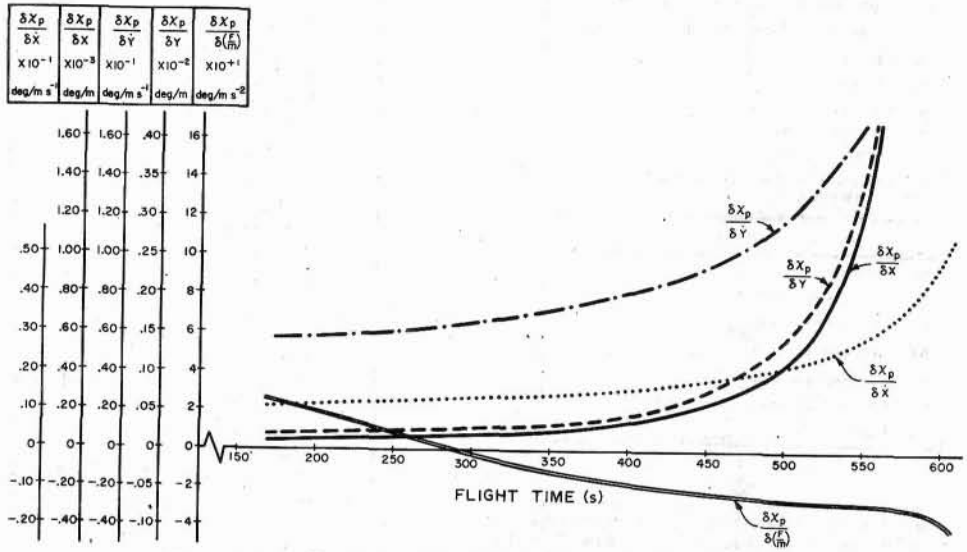

Figure 2.3-3. Sensitivity of the Guidance Parameter (Iterative Guidance).

2.4 Comparison of the Path Adaptive Polynomial Guidance Mode (PGM) and the Iterative Guidance Mode (IGM)

The overall guidance requirements for a given type of vehicle and its class of missions determine the most suitable guidance scheme. Both the PGM and the IGM schemes were designed to accommodate a large variety of missions including earth orbits, orbital changes, lunar flights, and deep space flights. The schemes were also designed for use with high thrust vehicles having one or more guided stages and for various vehicle configurations and characteristics. Historically, the PGM scheme was developed and flight tested first with excellent results. The IGM scheme was then developed to provide more flexibility with less preflight computation than the PGM. The IGM scheme was flight tested on Saturn SA-9 with excellent results and confirmed the predicted desirable characteristics of the scheme.

A prime requirement of any guidance scheme is its contribution to accuracy. This requirement

Table 2.3-1. Iterative Guidance Mode Equations Flight to Orbit.

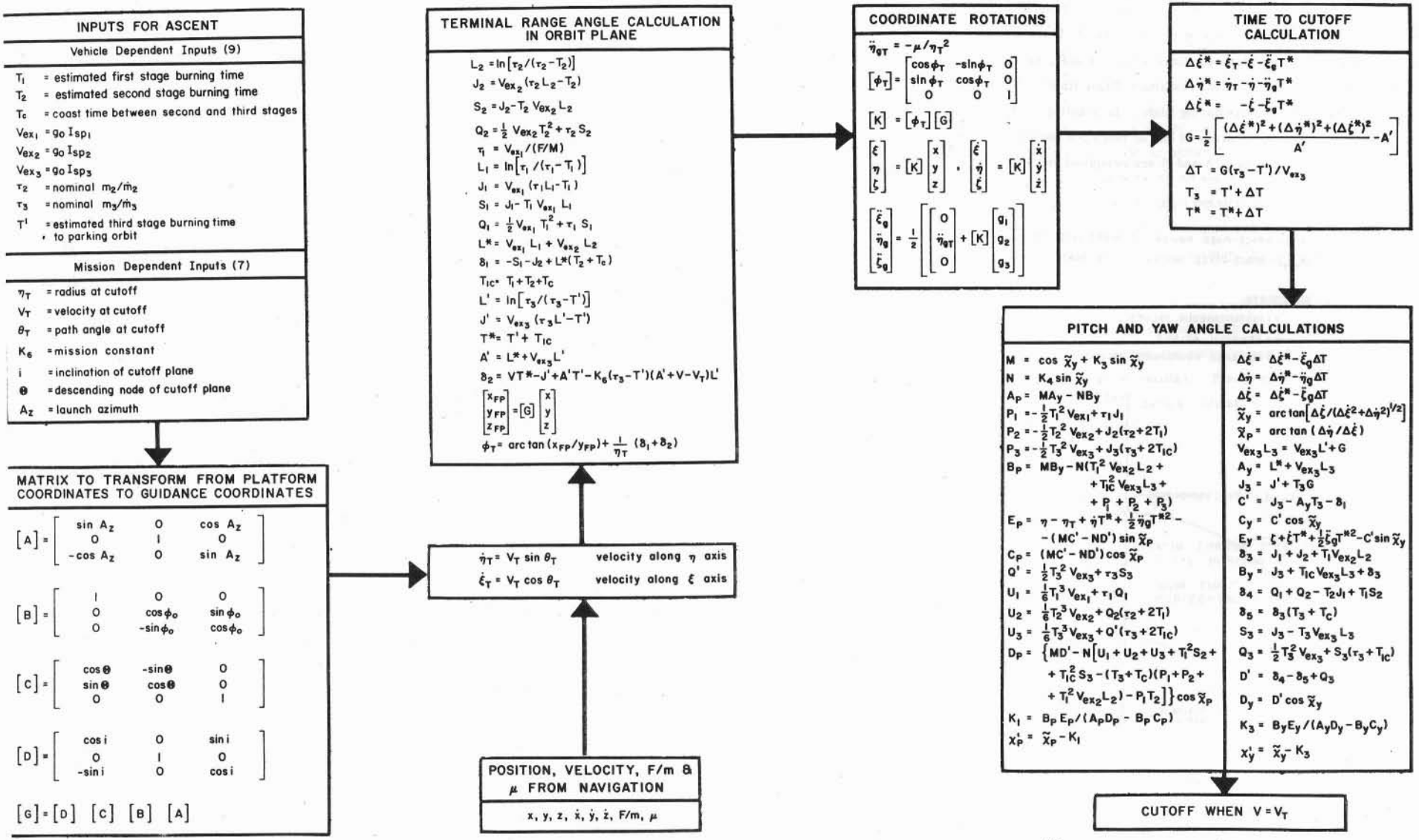

Table 2.3-2. Iterative Guidance Mode Equations Flight Out of Orbit.

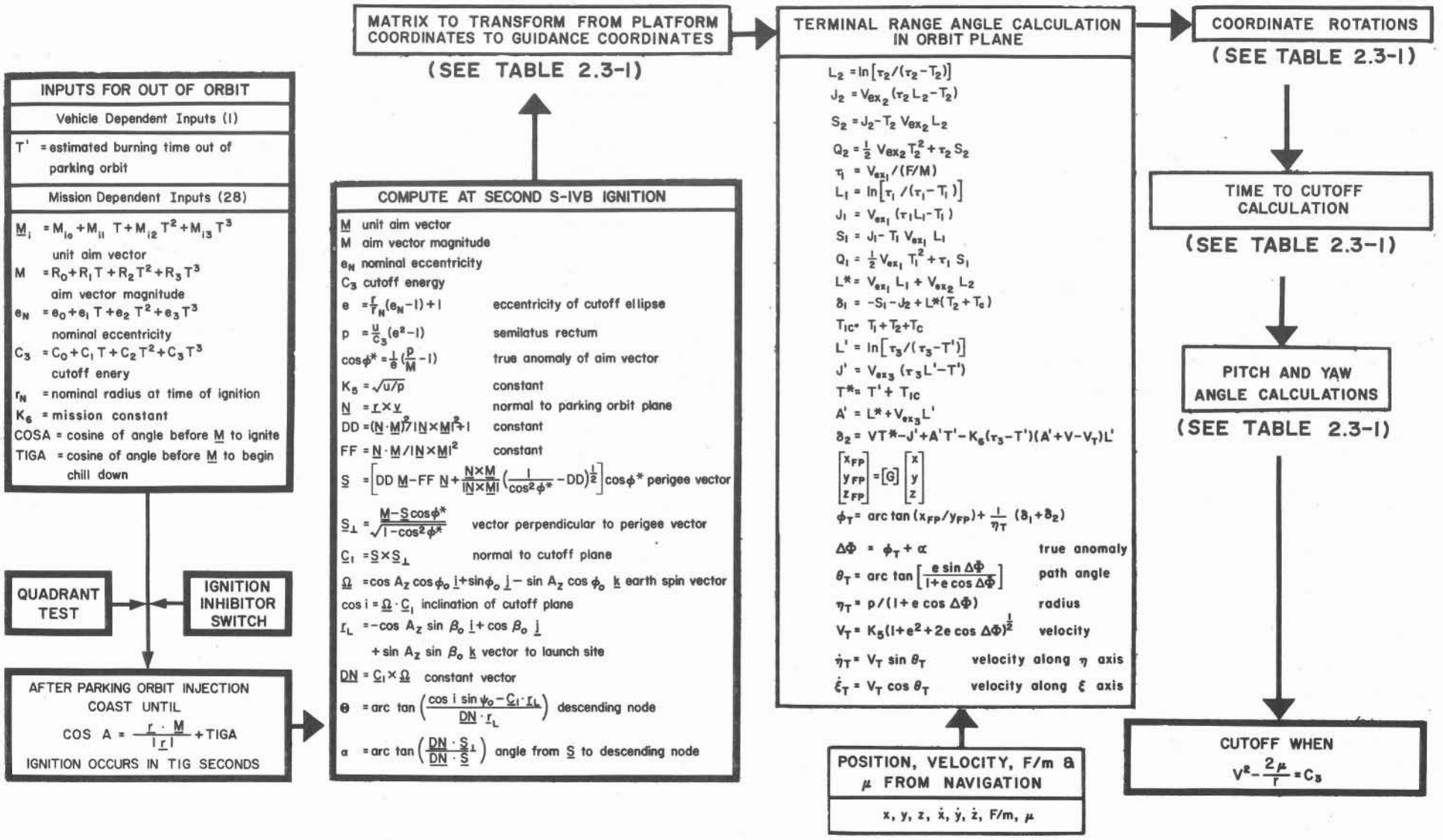

can be met satisfactorily by either scheme. Consequently, other characteristics of the schemes must be considered in making a comparison; they include the following.

(1) Preflight Computation Required. The number of precalculated trajectories required to generate the guidance equations or guidance presettings is a significant consideration when mission changes or changes in vehicle characteristics are to be expected as with the Saturn program. The reaction time to mission changes or changes in vehicle characteristics increases with the number of required precalculated trajectories. The PGM scheme requires approximately 100 to 300 precalculated trajectories, whereas only one or two precalculated trajectories are required to provide the presetting for the IGM scheme. This is a significant reduction in workload and preflight preparation time.

(2) Flight Computation Required. Generally, explicit guidance equations demand extensive onboard computation; practically, both IGM and PGM schemes require the same size, large digital flight computer.

(3) Mission and Vehicle Flexibility. The PGM guidance equations generally must be regenerated when mission or vehicle changes occur. The explicit IGM equations are valid for large mission changes and for vehicle modifications; only a few presettings need be changed for most applications. These equations can also be formulated to accommodate large launch windows with less difficulty than the PGM equations. The explicit equations of the IGM scheme are valid for any firing azimuth, and the presettings are easier to change with firing azimuth than the polynomial expressions of PGM that must be used in a general case.

(4) Propellant Economy. Minimum propellant trajectories that meet the mission requirements are computed with techniques of the calculus of variations. One trajectory is calculated for each expected inflight perturbation and the propellant consumption is tabulated. Corresponding trajectories are then computed using the actual guidance equations to direct the vehicle to the desired cutoff condition. The propellant consumption with each guided trajectory is then compared with the propellant consumption for the corresponding minimum propellant trajectory. The excess propellant required by the guided trajectories over that of the minimum propellant trajectories is a measure of the propellant economy of the scheme. When applied to a two stage vehicle designed to place a payload of approximately 11,000 kg in a low earth orbit, both the PGM and IGM schemes require only about 5 kg more propellant than the minimum propellant trajectory. Hence, both the IGM and the PGM scheme have excellent propellant economy.

In summary, both guidance schemes are satisfactory for the Saturn vehicles and missions. They give good accuracy and excellent propell[illegible] The principal advantages of the IGM scheme over the PGM are the increased flexibility in mee[illegible]g changes in missions and vehicles and

the relatively small amount of preflight computation required to generate the desired guidance presettings. In fact, the scheme comes very close to providing a single flight computer program capable of functioning for all orbital or lunar missions.

3. LAUNCH VEHICLE CONTROL

3.1 Introduction to Launch Vehicle Control Problems

During propulsion, the attitude control system must orient the thrust vector appropriately relative to the vehicle such that the required attitude commands are performed in a satisfactorily damped mode of rotation. Some of the problems arise because Saturn vehicles cannot be considered rigid but must be treated as distributed masses connected by an elastic structure. Forces acting on these masses resulting from atmospheric perturbations or active control of the vehicle excite the complex spring-mass system and cause body bending. Since the structure possesses low damping, oscillatory bending modes of considerable amplitude can be produced, to which control sensors may be subjected at their particular location. Thus incorrect information about the total vehicle behavior may cause self-excitation and instability of the vehicle control system.

Another problem is that the vehicles are aerodynamically unstable during most of the propelled flight in the atmosphere. As an example, Figure 3.1-1 is a plot of the center of pressure and the center of gravity for the first phase of the Saturn V and shows that the vehicle is unstable except for a short period of time around the 60th flight second.

The control system designer has further to consider that propellant sloshing exerts low frequency forces on the vehicle, and excitation through the control loop must be prevented. Also many vehicle characteristic data vary widely with time and the individual power stages; some can be predetermined only to a certain degree and tolerances must be imposed. Thus a wide operating range of the control system must be provided.

3.2 Vehicle Motion Equations [11]

For the control system synthesis and analysis, the vehicle motions must be available in the form of equations that serve as a mathematical model.

In establishing the equations, it is assumed that certain characteristic data can be treated as constants or slowly time varying functions and do not influence the characteristic modes of the control system for the time interval under investigation. Furthermore, terms of a negligible influence to the practical results are omitted.

The basic vehicle dynamics for small perturbations involve five basic ordinary linear differential equations.

(1) Moment balance equation for the rigid-body vehicle, coupled with sloshing mass and engine mass reactions.

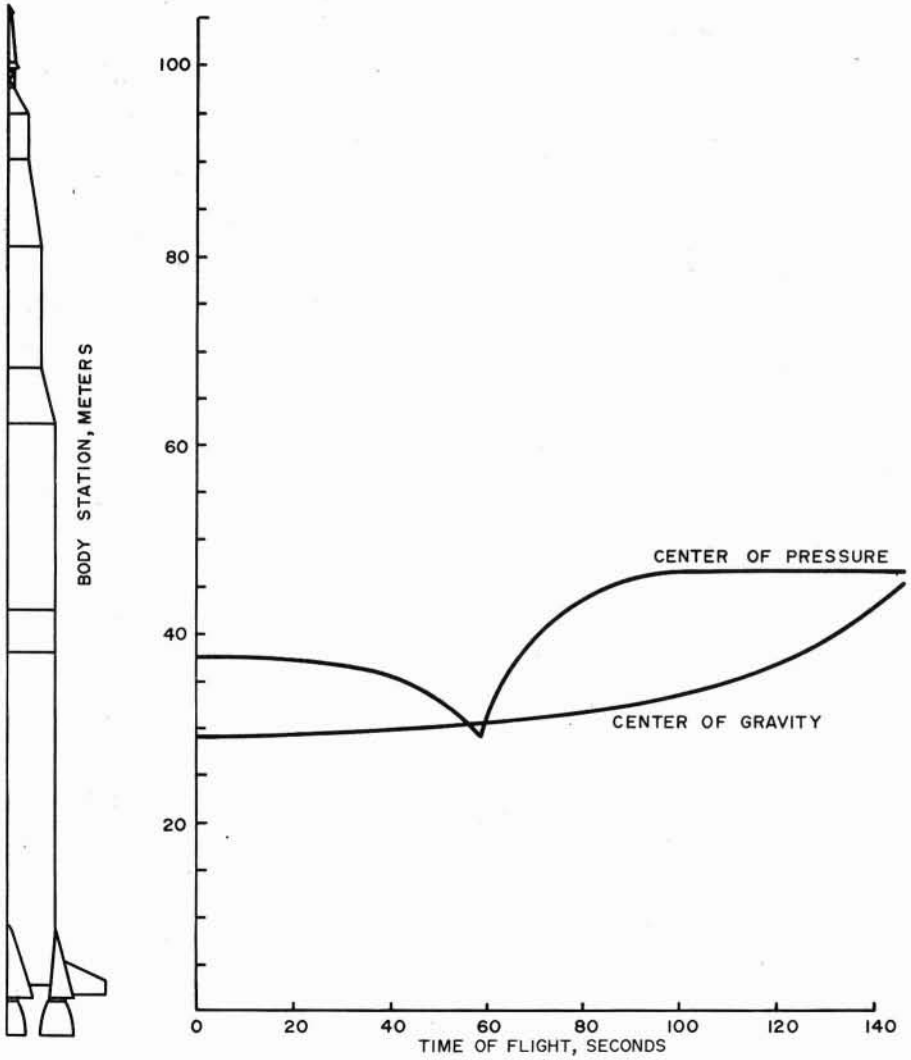

Figure 3.1-1. Variations of Center of Pressure and Center of Gravity During Flight.

(2) Force balance equation for the rigid-body vehicle, coupled with sloshing mass and engine mass reactions.

(3) Bending mode equations for the disturbed elastic vehicle structure, coupled with sloshing mass and engine mass reactions.

(4) Force balance equations for the propellant sloshing masses, coupled with rigid-body and elastic reactions.

(5) Angular relationships between rigid-body dependent variables.

In addition to these basic vehicle dynamics, other equations are introduced which define the dynamics of the control logic, engine, actuators, and control sensors.

3.3 Control Scheme and Equations

The development of the control scheme and its equations demands investigations in two areas: one covers the low frequency spectrum, consisting of the rigid-body control frequency and propellant sloshing; and the other covers the high frequency spectrum, consisting primarily of the bending modes, torsional modes, and compliance modes. After both areas have been analyzed, the effect of crosscoupling is examined and any necessary adjustments in the system are made. The complexity of the frequency spectrum as it exists, for example, on the Saturn V can be seen in Figure 3.3-1, which shows the basic frequencies during the first powered phase. The frequency bands are the results of changing vehicle state conditions because of propellant consumption as a function of flight time.

For Saturn V, the attitude/attitude-rate scheme is the basic control scheme and an accelerometer is added as needed to approach either drift-minimum or load-minimum conditions [12].

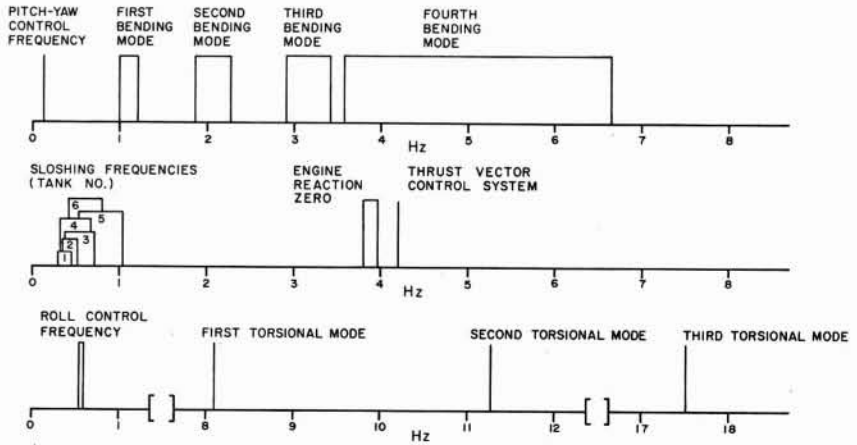

Figure 3.3-1. Frequency Spectrum During First Stage Propulsion.

The control law for an engine deflection β is

$$\beta = a_0 \Delta\phi + a_1 \dot{\phi} + g_2 \ddot{\gamma} \qquad (3.3\text{-}1)$$

where $\Delta\phi$ and $\dot{\phi}$ are the attitude error angle and the attitude rate and $\ddot{\gamma}$ is the lateral acceleration measured by a body mounted accelerometer with its sensitive axis perpendicular to the vehicle longitudinal axis; a_0, a_1, and g_2 are gain factors which must be properly selected to produce the drift-minimum or load-minimum condition.

The control accelerometer is rigidly attached to the vehicle and measures the acceleration normal to the vehicle axis. The acceleration measured by this control accelerometer differs from that measured by the guidance accelerometers, which are mounted on the stable platform and measure accelerations with respect to an inertial space coordinate system. In simplified mathematical terms, the acceleration sensed by the control accelerometer is

$$\ddot{\gamma} = \frac{N'}{m}\alpha + \frac{R'}{m}\beta + l_a \ddot{\phi} \qquad (3.3\text{-}2)$$

where the first term is the partial acceleration from an angle of attack, the second term results from the deflected thrust vector, and the third term is derived from the angular vehicle acceleration with l_a defined as the distance between the vehicle center of gravity and the body mounted accelerometer.

The design and selection of the control parameters for low frequency response is determined by consideration of several factors, such as:

(1) The rigid-body control frequency should be sufficiently below the frequency of the lowest bending mode to allow the design of shaping networks that stabilize the bending modes without adversely affecting the control mode.

(2) The control frequency must be high enough to provide adequate vehicle response and to minimize trajectory dispersions caused by thrust vector misalignment.

(3) The control gains, which determine the control frequency, must be high enough to guarantee that the operating point does not go below the static stability margin when tolerances in coefficients are included [13].

Typical tolerances used in designing the Saturn control systems are:

(1) ±0.3-caliber variation in the center of pressure location.

(2) ±20% of the normalized force coefficient $c_{z\alpha}$.

(3) ±0.15-caliber variation in the vehicle center of gravity.

(4) ±10% variation in the control gains.

(5) ±3% variation in engine thrust and/or loss of the thrust of an engine for multiple engine systems.

Requirements 1, 2, and 3 are to some degree conflicting, and the selection of the control frequency requires considerable evaluation and compromise before the final values are obtained. Thus during the first propulsion phase, the control frequency had to be chosen from 0.08 to 0.2 Hz. Simulator studies indicated that these values give reasonable dynamic response while lower values cause undesirably large dispersions in case of a thrust vector misalignment. The control frequency for the second stage burn is also approximately 0.15 Hz; however, this value was chosen mainly in view of first and second stage separation dynamics [14]. Preliminary indications are that the third stage control frequency will range between 0.2 and 0.4 Hz.

The selected control frequencies determine the control loop gains. Typical gain values for the Saturn V launch vehicles are given in Figure 3.3-2 and Table 3.3-1. The gains shown for the first stage flight are designed for drift-minimum control during the high aerodynamic pressure portion of flight. Changes in the attitude rate gain for the first stage, like the upper stages, will be by discrete steps. The attitude gain a_0 and accelerometer gain g_2 will be programed time varying functions.

Damping with respect to the sloshing modes is obtained by providing baffles in the propellant tanks. It has not been considered a practical solution to stabilize sloshing with the control system [15].

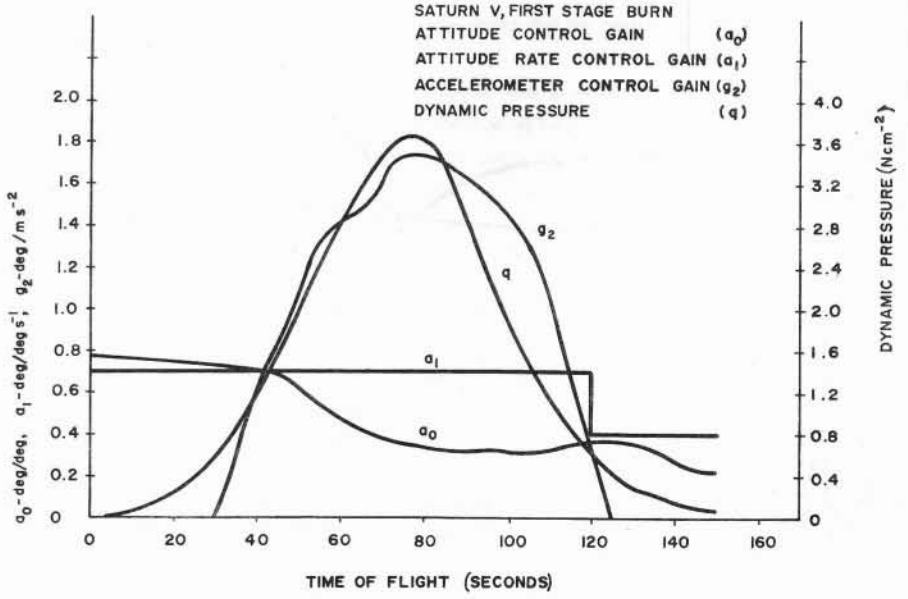

Figure 3.3-2. Gain Values for First Stage Flight.

Table 3.3-1. Saturn V Control Gains.

Second Stage Propulsion Period		
t(seconds	a_o(deg/deg)	a_1 (deg/deg s^{-1})
0 - 200	1.7	3.4
200 - 330	0.7	1.0
330 - 390	0.3	0.45
Third Stage Propulsion Period		
t(seconds)	a_o(deg/deg)	a_1 (deg/deg s^{-1})
0 - 395	2.0	1.85
395 - 469.5	2.0	1.30

Stabilization of the Saturn vehicles with respect to bending and torsion modes is achieved by shaping networks in each of the three control sensor channels. During first stage operation, the first and second bending modes are very close to the control loop frequency; therefore, they will be phase stabilized, whereas higher modes will be attenuated. During the second stage powered flight, only the first bending modes will be phase stabilized and higher modes will be attenuated. The bending mode frequencies during third stage powered flight are higher than those for the other stages; therefore, all the bending modes of this stage will be stabilized by attenuation. All torsional modes are at a relatively high frequency and will be attenuated for all stages.

To provide the desired phase, it is necessary that the rate gyro be properly located on the vehicle. Figure 3.3-3 exhibits the Saturn configuration and the first two bending mode shapes. An examination of this figure shows that two accessible areas exist where the slopes of the first and second bending modes have the same sign. One area is toward the rear of the vehicle and the other is in the S-II/S-IVB interstage area.

Location of the rate gyro in the rear area of the vehicle would require phase lead of the rate gyro signal towards the vehicle attitude to stabilize the first and second modes. This makes the stabilization of the higher modes difficult, as attenuation is inherently associated with phase lag. If the rate gyro is located in the S-II/S-IVB interstage area, attenuation of the higher modes will be easier because the first two bending modes will require phase lag from the shaping network.

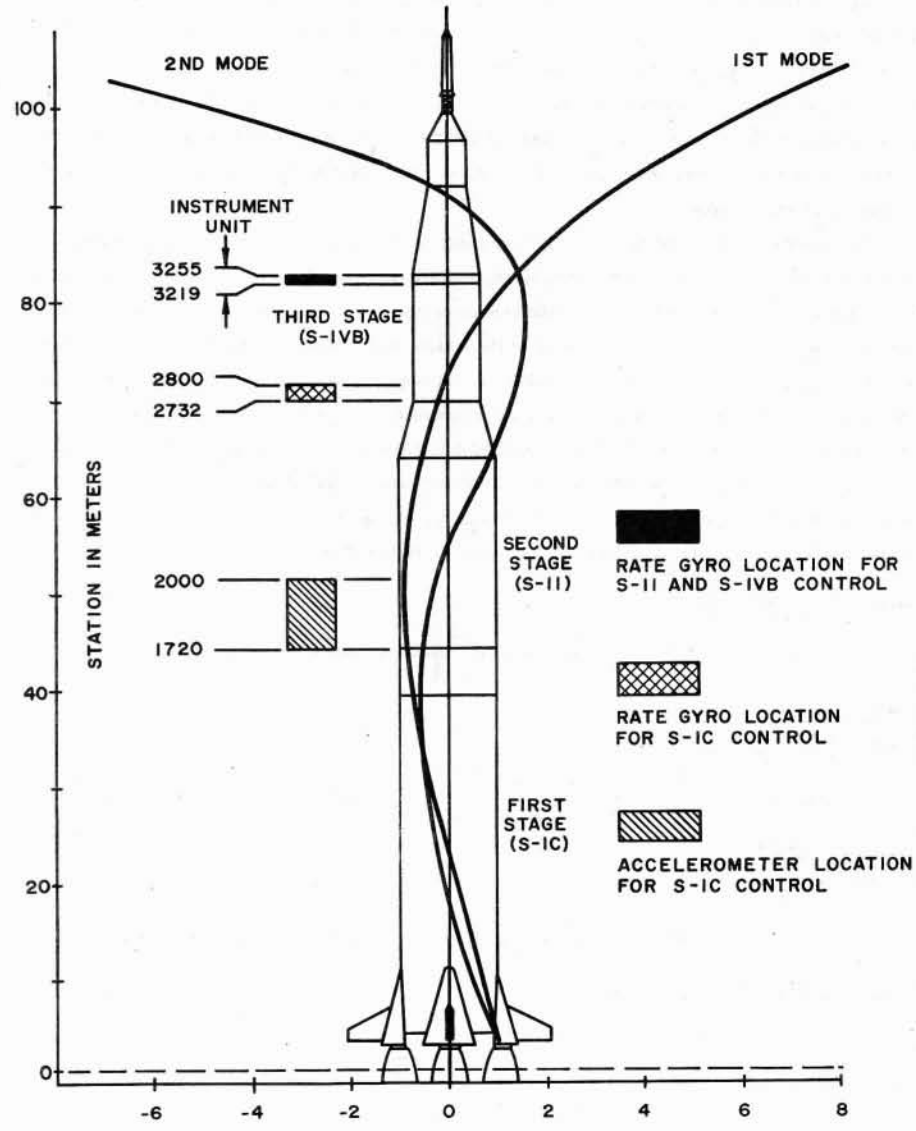

Figure 3.3-3. Shape of the First and Second Bending Modes.

The same argument holds for selection of the rate gyro for the second stage propulsion phase although only one mode will be phase stabilized. By placing the rate gyro in the Instrument Unit, phase lag will be required in the shaping network for both stages.

As noted earlier, the attitude gyro is located in the Instrument Unit. Since the control loop gain at the bending mode frequencies is much less through the attitude loop than through the rate loop, the location of the attitude gyro is not as sensitive and is determined by the need to have one centrally located unit for all stages.

The location of the body mounted accelerometer (used only in the first stage propulsion phase) is determined by two factors. First, rigid-body stability analyses limit the distance the sensor can be located in longitudinal direction from the vehicle center of gravity. Second, the phase sensed by the accelerometer when located to the rear of the vehicle center of gravity subtracts from the rigid-body lead margin. Two locations are provided for this sensor, one in the forward section of the first stage and one in the tail section of the third stage; the final location will be selected after evaluation of the dynamic test of the vehicle. The simplified block diagram shown in Figure 3.3-4 illustrates the basic partial control loops, one for each control sensor. $F(\Delta\phi)$, $F(\dot{\phi})$, and $F(\ddot{\gamma})$ are the shaping networks necessary to stabilize the vehicle and a_0, a_1, and g_2 are the total control gains illustrated earlier. Figure 3.3-5 shows typical shaping networks and their transfer functions.

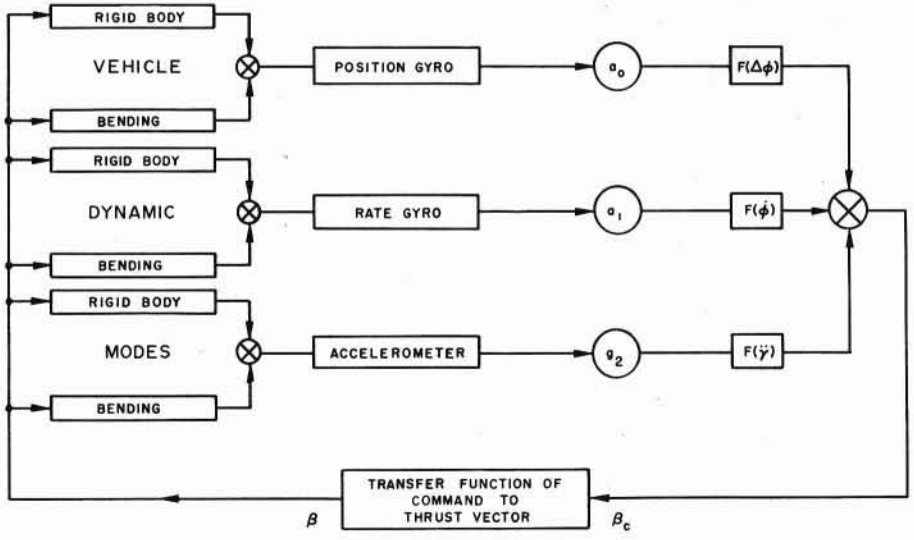

Figure 3.3-4. Block Diagram of the Control Loop.

PITCH-YAW ATTITUDE ERROR CHANNELS

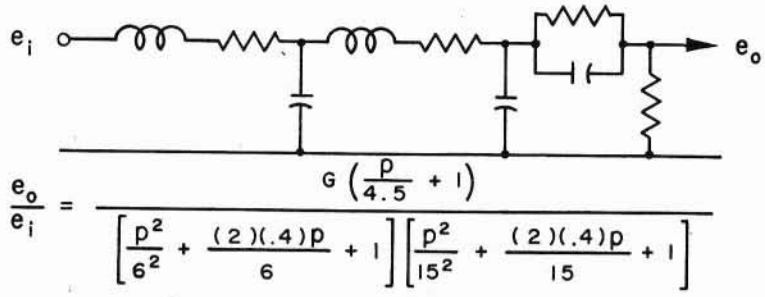

$$\frac{e_o}{e_i} = \frac{G\left(\frac{p}{4.5}+1\right)}{\left[\frac{p^2}{6^2}+\frac{(2)(.4)p}{6}+1\right]\left[\frac{p^2}{15^2}+\frac{(2)(.4)p}{15}+1\right]}$$

PITCH-YAW ATTITUDE RATE CHANNELS

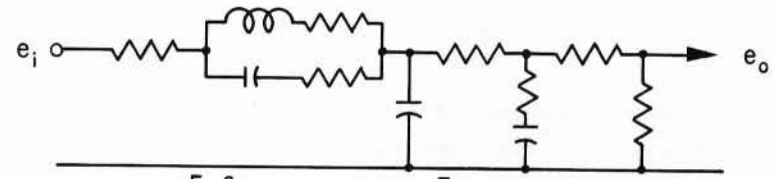

$$\frac{e_o}{e_i} = \frac{G\left[\frac{p^2}{15}+\frac{(2)(.4)p}{15}+1\right]}{\left[\frac{p}{5}+1\right]\left[\frac{p^2}{6^2}+\frac{(2)(.3)p}{6}+1\right]}$$

PITCH-YAW ACCELEROMETER SIGNAL CHANNELS

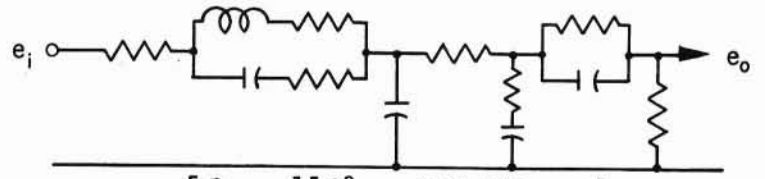

$$\frac{e_o}{e_i} = \frac{G\left[\frac{p}{4}+1\right]\left[\frac{p^2}{112}+\frac{(2)(.3)p}{11}+1\right]}{\left[\frac{p}{2.5}+1\right]\left[\frac{p^2}{3^2}+\frac{(2)(.4)p}{3}+1\right]\left[\frac{p}{50}+1\right]}$$

Figure 3.3-5. Shaping Networks.

3.4 Vehicle Attitude Control During Coast and Low Thrust Phases

Figure 3.4-1 depicts the auxiliary propulsion control loop for the third stage of Saturn V, and Figure 3.4-2 shows the switching logic used. As shown on the diagram, the system has both angular position and angular rate feedback.

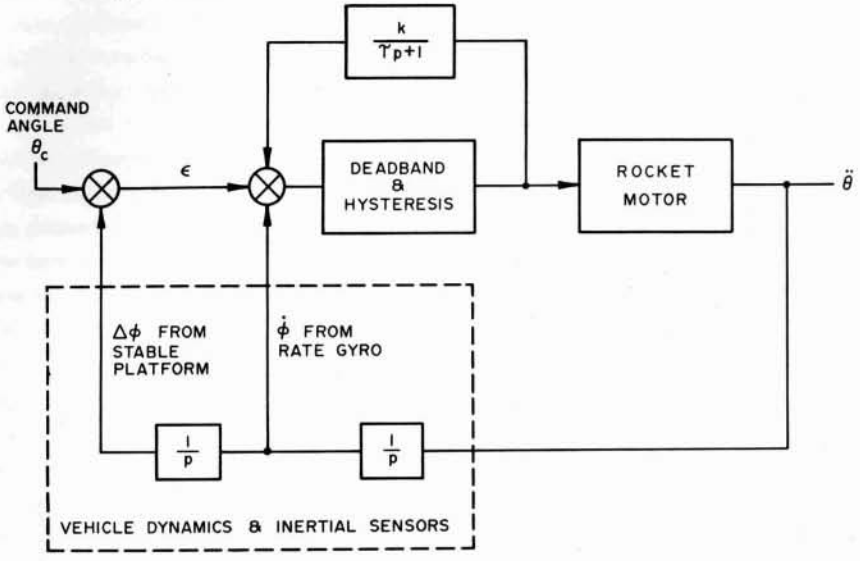

Figure 3.4-1. Auxiliary Propulsion Control Loop.

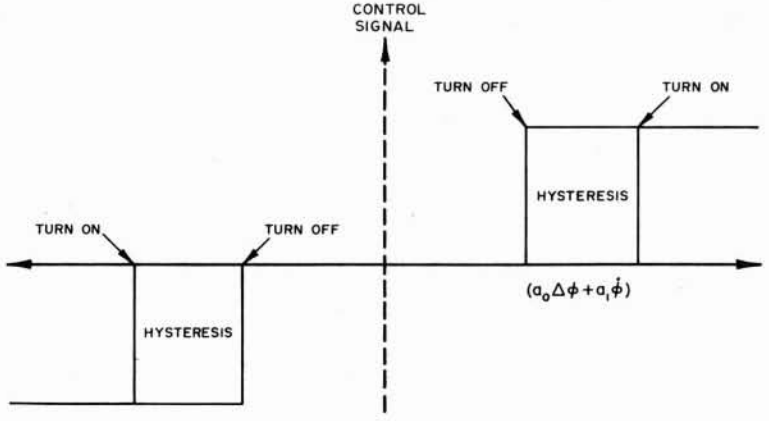

Figure 3.4-2. Switching Logic.

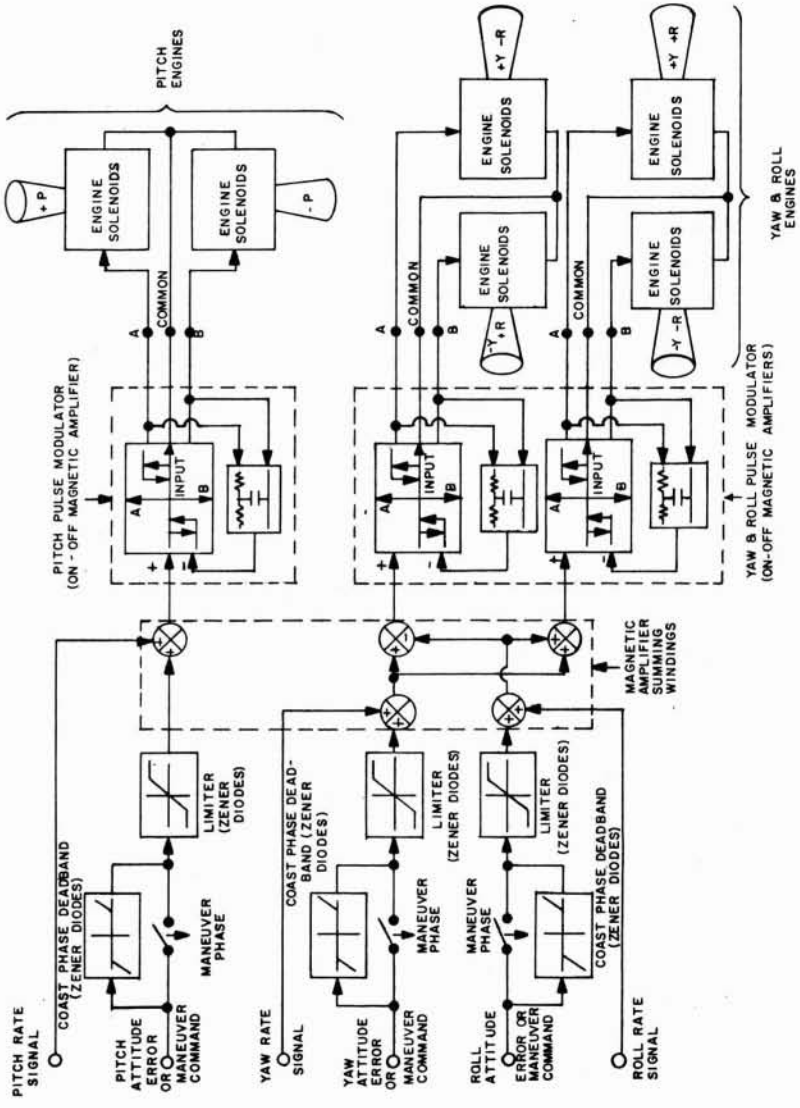

Figure 3.4-3. Spatial Attitude Control System.

Figure 3.4-3 depicts the three-axis scheme for attitude control during coast or low thrust conditions.

To fulfill the requirement that the engines produce thrust pulses of either short or long duration, pulse modulators utilizing switching magnetic amplifiers are used to actuate the engine solenoids. Over a certain range of the pulse modulator input signal, the output of each magnetic amplifier is both pulse width and pulse frequency modulated as a function of the input signal. Below this range, the amplifier output is OFF and, above this range, it is continuously ON. Output A is positive for a positive input signal and output B is positive for a negative input signal; both outputs are of sufficient voltage magnitude to actuate the engine solenoids. To provide this type of operation, each magnetic amplifier has a preset amount of deadspace, a specified amount of switching hysteresis, and a first order lag feedback with a polarity (relative to the input signal) as shown in Figure 3.4-2. Both the amount of switching hysteresis and the feedback network characteristics are sized to insure minimum impulse operation of the particular engines used.

The amplifier deadspace is adjusted for a permissible amount of control system attitude or attitude rate deadband.

4. SATURN LAUNCH VEHICLE HARDWARE DESCRIPTION

4.1 Overall System and Signal Flow

Figure 4.1-1 exhibits the flow of signals and the main components of the guidance and control system. Vehicle attitude and acceleration are measured by the inertial platform and its accelerometers, converted to digital form by the data adapter, and processed by the digital guidance computer.

According to the preprogramed guidance equations, the guidance computer determines cutoff time and control command signals, which are converted from digital to analog in the data adapter. Timed signals and cutoff are processed to the digital switch selectors in the various vehicle stages. The data adapter can also accept signals from the command receiver to select alternate guidance and control modes and to update information.

The analog control computer shapes, mixes, and amplifies the guidance signals from the data adapter, damping signals from the rate gyros, and control accelerometer information for angle-of-attack control. Alternate guidance and control commands can be taken from the spacecraft instrumentation or from manual control. The summed command signals are furnished to the actuators of the various vehicle stages.

The following sections describe in detail the major items of equipment performing guidance and control in the Saturn booster.

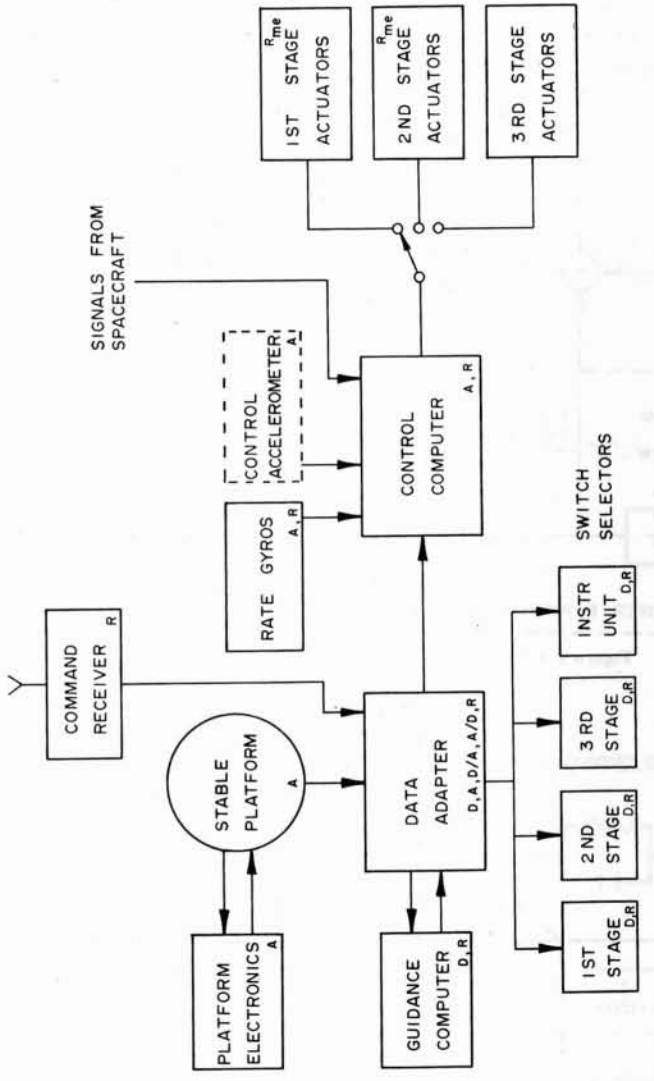

Figure 4.1-1. Guidance and Control Flow Diagram.

4.2 Stable Platform [16]

The ST124-M inertial platform system provides the integrated acceleration data, inertial reference coordinates, and vehicle attitude measurements with respect to these coordinates for guidance and control of the Saturn space launch vehicle. The system consists of two major assemblies, the stable platform and the platform servoamplifier. The solid state electronics to close the platform gimbal servoloops, the accelerometer servoloops, and an impulse function generator for automatic checkout of each servoloop are contained in the platform servoamplifier.

The stable platform (Fig. 4.2-1) is designed so that it can be built as a three or four gimbal platform, depending on the mission requirements. For the present version of the Saturn V/Apollo, the three gimbal platform is sufficient. The inner gimbal of the platform is stabilized by three mutually perpendicular single-degree-of-freedom gas bearing gyros mounted on the inner gimbal with their input axes aligned along an orthogonal coordinate system X, Y, and Z. The output axes of the gyros have been oriented with respect to the main thrust vector for minimum error contributions by anisoelastic effects. The inner gimbal further carries three gas bearing pendulous integrating gyro accelerometers with their input axes aligned along the orthogonal coordinate system X, Y, and Z. The measuring head of each accelerometer contains a pendulous single-degree-of-freedom gyro; the position of the measuring head relative to the stable frame is a measure of integrated acceleration along the input axis of each accelerometer.

The platform orientation system will align the y vector along the launch local vertical; the y vector points outward from the earth's surface. The laying system will position the inner gimbal in azimuth so that the X vector will point in flight direction and the plane formed by the X, Y axes will be parallel to the desired flight plane.

The Z accelerometer that measures perpendicular to the flight plane will provide cross-range guidance. The X and Y accelerometer information will be used to obtain the pitch attitude of the vehicle acceleration vector and the required cutoff velocity.

Figure 4.2-2 is a block diagram of the platform gimbal servoloop. The servoloops use a 4.8 kHz amplitude modulated carrier system with the gyro outputs amplified and demodulated on the gimbals of the platform. The dc signal is shaped in a stabilization network, remodulated at 4.8 kHz, amplified, and then demodulated prior to entering the dc power bridge. This dc power bridge provides a current source drive for the direct axis dc gimbal torquer to obtain a servoloop independent of torquer heating and commutator brush resistance. A 4.8 kHz carrier was chosen to provide sufficient bandwidth for the servoloop.

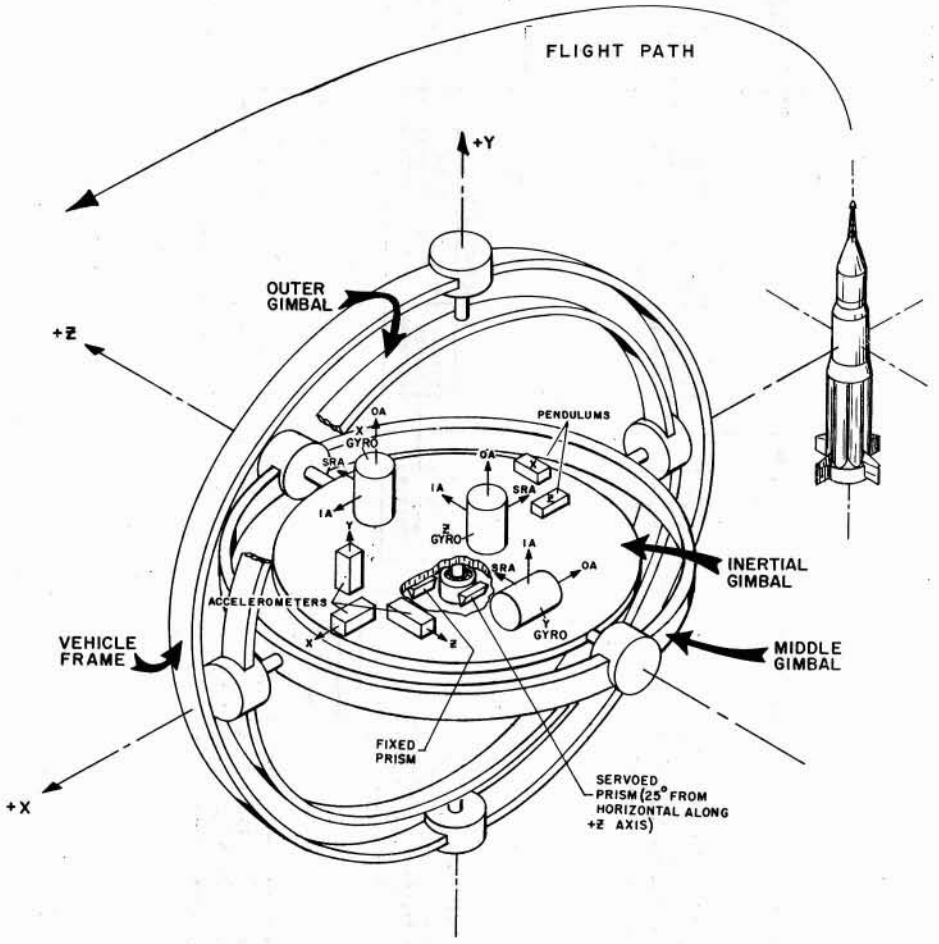

Figure 4.2-1. Stable Platform.

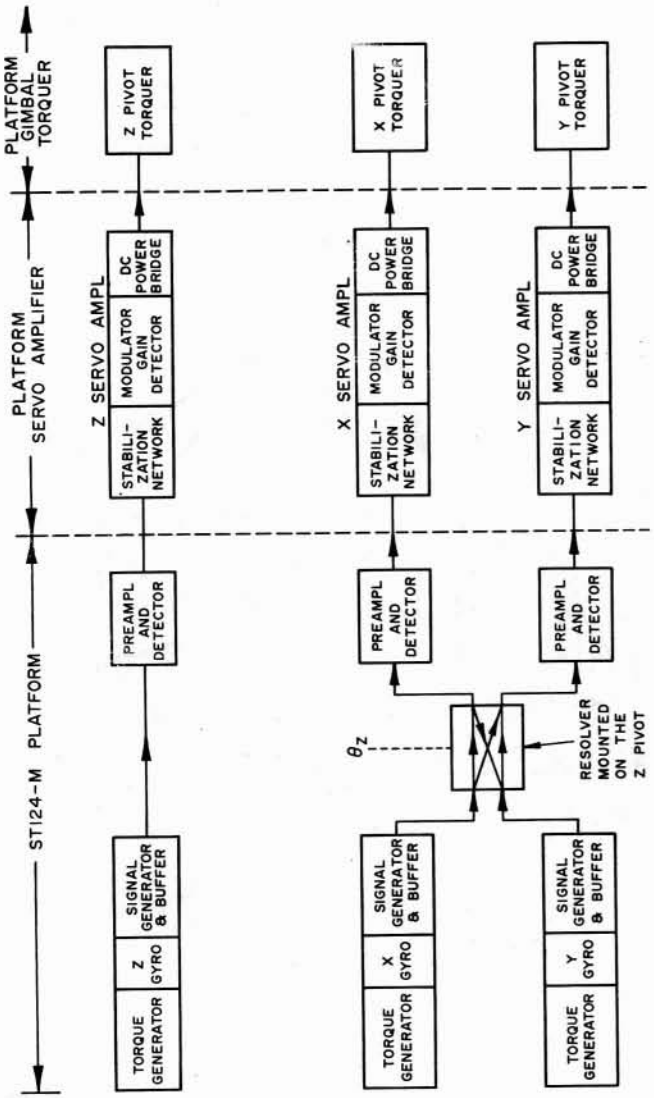

Figure 4.2-2. Gimbal Servoloops.

The Z servoloop has the Z gyro output signal phase shaped and amplified in the servoamplifier and sent to the Z pivot torquer (the innermost pivot of the platform) as shown in Figure 4.2-2. The X and Y gyro output signals are resolved along the X and Y coordinates of the middle gimbal by a resolver mounted along the Z or inner pivot. These outputs of the resolver are preamplified and demodulated on the middle gimbal. The signal to the X servoamplifier is further amplified and fed to the X or middle pivot torque generator while the Y servoamplifier drives the Y or outer pivot torquer. No gain compensation such as secant θ_X is used in the Y servoloop for middle gimbal angles $-45° < \theta_X < 45°$.

The servoloop signals to and from the platform are dc signals and are at a level high enough to neglect slip ring noise and resistance variations. The use of dc transmission was chosen to eliminate pickup and cable problems.

Analog resolvers are used for angular readouts; the phase shifts of their output voltages are measured by digital techniques. This method has been preferred to direct digital readout, for which the present state of the art is not considered to be sufficiently advanced with respect to accuracy and size.

For the demanded high readout accuracy, dual resolvers are used. They possess two independent two-phase windings in the same magnetic structure, one for one-pole-pair and one for multiple-pole pairs.

Prior to launch, the stable platform must be oriented into the measuring directions of the accelerometers. In principle, this orientation could be carried out with the ξ and ζ accelerometers responding to the gravitational acceleration. However, the pendulous integrating accelerometer delivers the integrated acceleration; this signal has a 90-degree phase lag against the actual acceleration and is disadvantageous for the erection servo control loop. Therefore, direct-measuring accelerometers in the form of gas bearing supported pendulums are preferable. In addition to their primary purpose, i.e, to sense deviations from the local plumb line, they are useful to cross-check the ξ and ζ accelerometers. Thus two pendulums are mounted on the platform inner gimbal and are used to erect the platform to the local vertical.

For azimuth alignment, the inner gimbal contains a fixed prism and a servo-driven prism (Fig. 4.2-1). The fixed prism has its porro edge parallel to the X axis while the porro edge of the movable prism rotates in the X, Z plane. The movable prism is driven by a geared servomotor mounted to the inner gimbal through a gear train of 10^5:1, and the angle between the prism and the inner gimbal is measured by a dual-speed control transmitter synchro.

The azimuth alignment block diagram is shown in Figure 4.2-3. After the inner gimbal is erected to the launch vertical, the baseline azimuth is obtained by closing the encoder repeater servo through contact D and the Y gyro alignment loop through contact A.

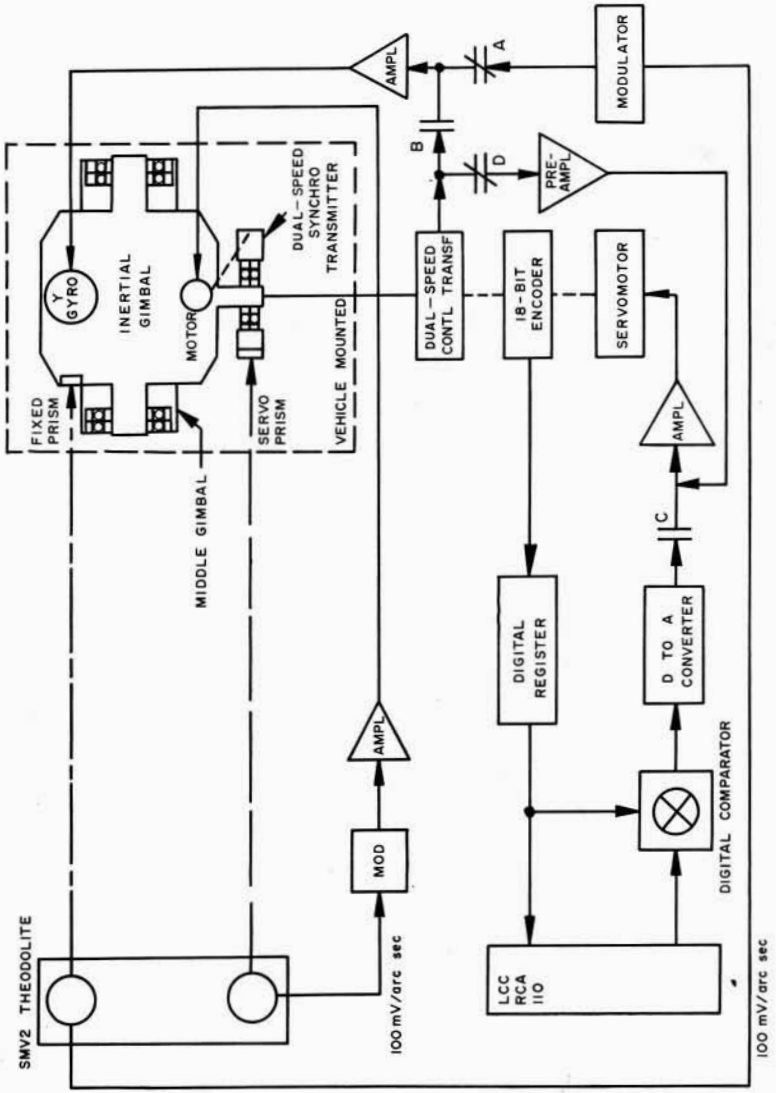

Figure 4.2-3. Azimuth Alignment Scheme.

The fixed prism error signal is transmitted from the theodolite through contact A to the Y gyro alignment loop, which will position the inner gimbal to the reference azimuth. At the same time, the servoed prism error signal from the theodolite will drive the servomotor on the inner gimbal to align the movable prism along the same baseline. The encoder servo will follow the dual-speed synchro on the inner gimbal and the 18-bit encoder signal will be stored in the ground based digital computer. This stored signal is a calibration of the zero alignment to eliminate transmission errors in the synchro system.

The mission azimuth is established by opening contacts A and D and by closing contacts B and C. The ground based digital computer determines the mission azimuth and directs the 18-bit encoder to its desired shaft position. The error signal from the dual-speed synchro system is fed to the Y alignment loop and drives the inner gimbal to its mission azimuth as the servoed prism is held fixed with respect to the optical beam from the theodolite or baseline azimuth.

The laying system has an accuracy of ±20 arc seconds.

4.3 Gas Bearing Gyro [17]

The cylindrical externally-pressurized gas bearing provides an almost torque-free support for the single-degree-of-freedom gyro. An obvious advantage of this support is that the weight and therefore the angular momentum of a certain size gyro are not limited by average density requirements for the float as in the case of the liquid flotation bearing. Consequently, maximum angular momentum with respect to gyro size and high structural stiffness can be obtained; for specified accuracy, comparatively high perturbation torques are possible. Furthermore, modest temperature limits can be imposed to obtain constant accuracy; no need exists to compensate or recalibrate for bias torques.

The gas bearing gyro (type AB5-K8) is shown in a cutaway view in Figure 4.3-1. Details of the gas bearing assembly are displayed in Figure 4.3-2. Pressurized dry nitrogen gas enters the gap between the cylinder (which contains the gyro motor and flywheel) and the sleeve through two rows of millipore discs, which act as flow restrictors and provide the bearing stiffness. The gas flows symmetrically to both end plates and escapes around the center openings of these end plates. Thus the cylinder is supported in radial and axial directions.

The signal and the torque generators are of the ac type to avoid magnetic remanent torques, which could occur from dc excitation. The signal generator is a shorted single winding sensor for the angular displacement of the gyro about its output axis. The torque generator operates like an eddy current motor and provides only alignment torques for initial erection.

Some gyro characteristics are shown in Table 4.3-1.

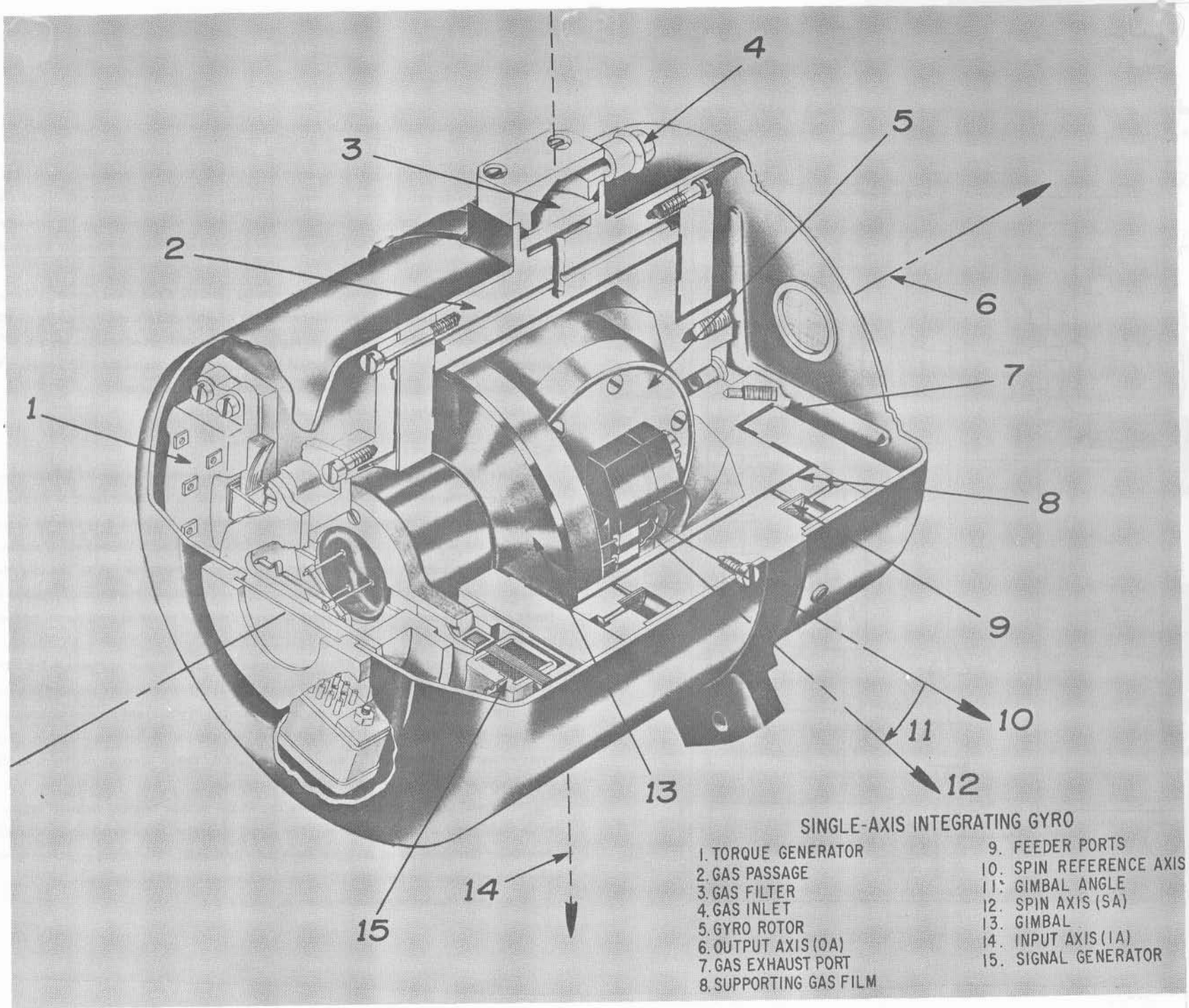

Figure 4.3-1. Gas Bearing Gyro.

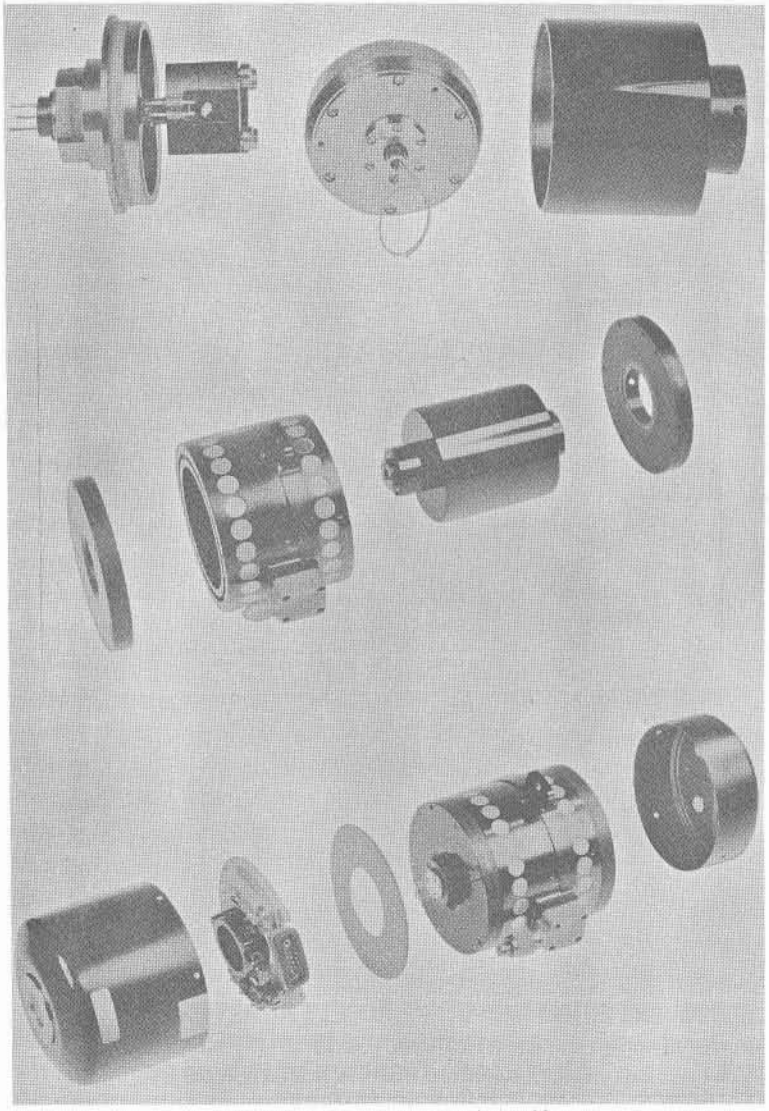

Figure 4.3-2. Gas Bearing Assembly.

Table 4.3-1. Characteristic Data of the Gyro and Accelerometer.

Item	Dimension	Gyro	Accelerometer
Gyro Wheel			
Type		synchronous hysteresis	synchronous hysteresis
Angular momentum	[$cm^4\ g\ s^{-1}$]	2×10^6	1×10^5
Wheel speed	[rpm]	24,000	12,000
Wheel excitation and power at 26 V, 3 phase 400 Hz	[W]	8	4.5
Gas Bearing			
Gas pressure	[$N\ cm^{-4}$]	10	10
Gas flow rate	[cm^3/min]	2000	2400
Air gap	[cm]	.0015 to .002	.0015 to .002
Sleeve, end plate, and cylinder material		anodized beryllium	anodized beryllium (end plate Monel)
Signal Generator			
Type		2 pole shorted turn reluctance	4 pole shorted turn reluctance
Excitation (4.8 kHz)	[V]	10	10
Sensitivity	[mV/deg]	550 with 10 kΩ load	285 with 10 kΩ load
Float freedom	[deg]	±3	±3
Torquer			
Type		shorted turn reluctance	direct axis dc torquer
Normal erection rate	[deg/min]	6	
Maximum torque	[cm kg]		1.44
Physical Characteristics			
Size	[in.]	3 dia. by 4 length	3.25 dia. by 5 length
Mass	[g]	900	1200
Velocity Pickoff - Optical Encoder (redundant output)			
Scaling	[$m\ s^{-1}\ rev^{-1}$]		300
Resolution	[$m\ s^{-1}$/bit]		0.05

4.4 Pendulous Integrating Gyro Accelerometer with Gas Bearing [17] (Fig. 4.4-1)

The gyro motor and flywheel of the gyro accelerometer are shifted along the spin reference axis to obtain the desired pendulosity about the gyro output axis. The gas bearing containing the gyro is mounted to rotate freely about the gyro input axis, which points in the measuring direction. A signal generator measures angular deflections of the gyro about the output axis and controls the servomotor on the gyro input axis. The precession angle is read out with high accuracy by an optical encoder with redundant readout.

A constant accelerometer scale factor, defined as velocity increment per revolution about the input axis, is guaranteed by a synchronous spin motor supplied from a power source with crystal-controlled frequency. To reduce temperature dependency of the scale factor, mechanical temperature compensation is applied. An increase in pendulosity with temperature is balanced by the change in angular momentum caused by the expansion of the gyro flywheel with increasing temperature.

Table 4.3-1 shows some characteristic data of the pendulous integrating gyro accelerometer.

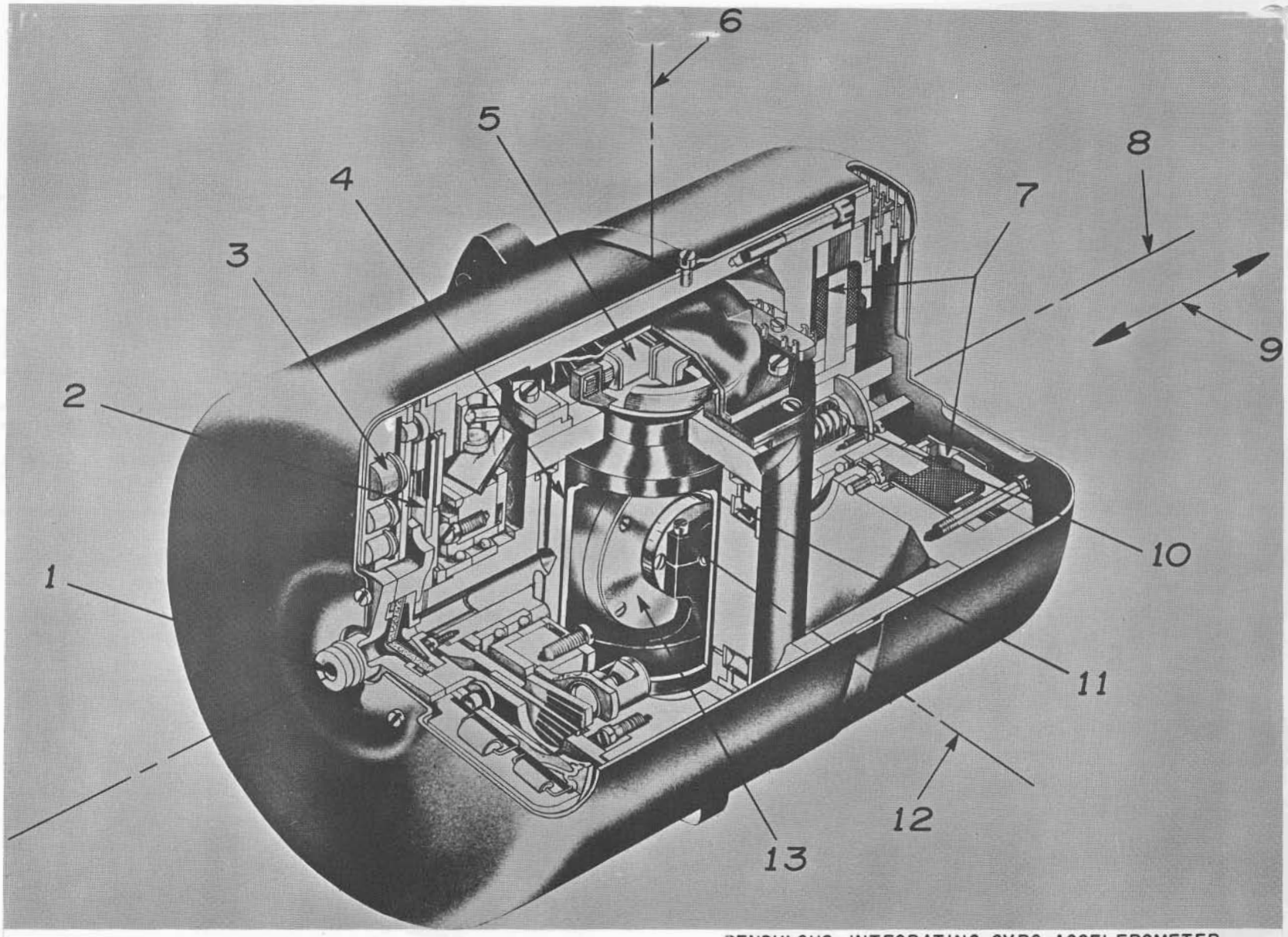

PENDULOUS INTEGRATING GYRO ACCELEROMETER

1. GAS INLET
2. ENCODER DISCS
3. ENCODER ELECTRONICS
4. SUPPORTING GAS FILM
5. SERVO PICK OFF
6. GYRO OUTPUT AXIS
7. TORQUER
8. GYRO INPUT AXIS
9. ACCELEROMETER MEASURING DIRECTION
10. SLIP RING CAPSULE
11. FEEDER PORTS
12. SPIN REFERENCE AXIS
13. GYRO ROTOR

Figure 4.4-1. Pendulous Integrating Gyro Accelerometer.

4.5 Digital Computer and Data Adapter

4.5.1 Functions

The launch vehicle digital computer and the launch vehicle data adapter fulfill the computational and input/output requirements for the Saturn V launch vehicles. These units, which represent one of the first applications of redundancy techniques in a large scale to operational hardware, also assist in the ground and orbital checkout of the booster and spacecraft. The phases of operation of the system may be considered in the sequence; prelaunch checkout, launch vehicle guidance, orbital checkout, and translunar injection.

During prelaunch checkout [18], the Saturn V system will be checked automatically through command from the ground launch computer. The onboard digital computer and data adapter system, in conjunction with the ground launch computer, will be utilized to check itself as well as to assist in the checkout of other subsystems in the Instrument Unit (IU), such as the platform accelerometers and gimbal angles, the vehicle switch selector, and the radio command receiver. Furthermore, any measurement normally telemetered from the IU or the third stage can be monitored through the computer. Before launch, all communication between onboard and ground support equipment is handled through the ground launch computer and/or the telemetry system. The ground launch computer sends test variables to the airborne computer, which performs test operations as required from the information and sends the results back to the ground launch computer via telemetry for verification. Guidance constants are loaded in and read back for verification. Test programs are contained in the computer for each mode, and a sequence simulating the actual mission is carried out to check parts of each program.

The computer performs the calculations for navigation and guidance required for the launch vehicle. During the major computation cycle (navigation and guidance loop), the instantaneous position and the velocity vector are determined, and the required velocity direction is computed according to a path adaptive scheme. The gravitational acceleration is computed and combined with the measured velocity, and coordinate resolution utilizing platform gimbal angles is accomplished. These computations have a repetition time of approximately one second. In the attitude correction or minor computation loop, commands are computed at a rate of approximately 25 times per second (Fig. 4.5.1-1).

In earth orbit, the digital computer serves again to check out the IU as well as the propulsion, attitude control, radio command, guidance, and telemetry subsystems. The computer and data adapter sequentially initiate stimuli to each system and compare the telemetry data with prestored go/no-go values. Any IU or third stage measurement that is telemetered can be read by the computer and data adapter. Data and control information necessary for checkout may be inserted into the computer from the ground via the radio command link.

The computations required for translunar injection are similar to those used for guidance into earth orbit.

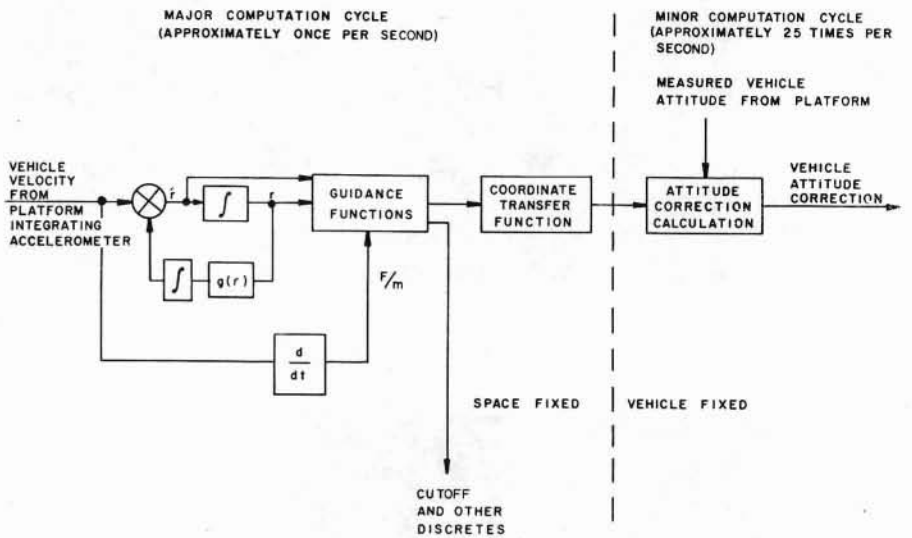

Figure 4.5.1-1. Major and Minor Computation Loops.

The data adapter interconnects the digital computer, the main guidance and control components, the switch selectors, the telemetry system, the power supplies, the ground launch computer, and the peripheral IU equipment; digital-to-analog and analog-to-digital conversion is included in this interconnection assignment.

The computer system utilizes microminiature packaging techniques as far as feasible. Semiconductor chips are mounted on square ceramic wafers (side length 7.5 mm) on which interconnecting wiring and film resistors have been deposited by silk screen printing and firing. The devices, called unit logic devices, are soldered to multilayer interconnection boards. Each multilayer interconnection board has a capacity of 35 unit logic devices. Two multilayer interconnection boards are bonded back-to-back to a supporting metal frame to form a logic page assembly. Multilayer interconnection boards and pages are joined by connectors to a central multilayer printed circuit board (Figs. 4.5.1-2 and 4.5.1-3).

For applications requiring extreme accuracy or large drive current capability, circuit modules composed of conventional discrete components are utilized. These find greatest application in the data adapter but are also used in the computer as memory drivers. The circuit modules are

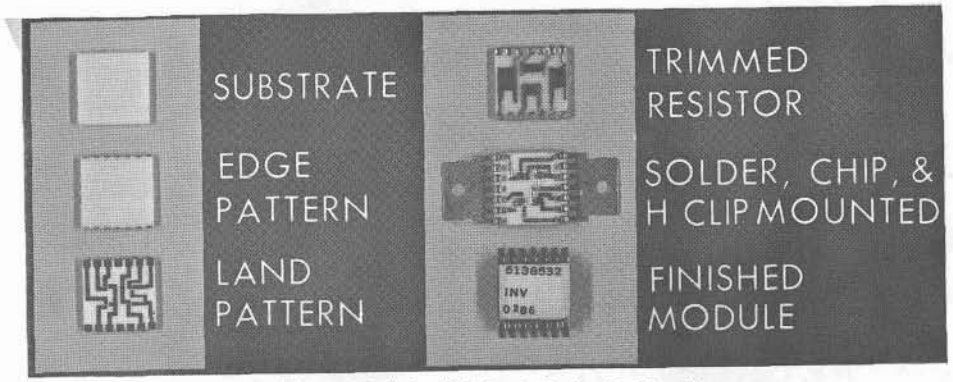

Figure 4.5.1-2. Unit Logic Device Buildup (Actual Size).

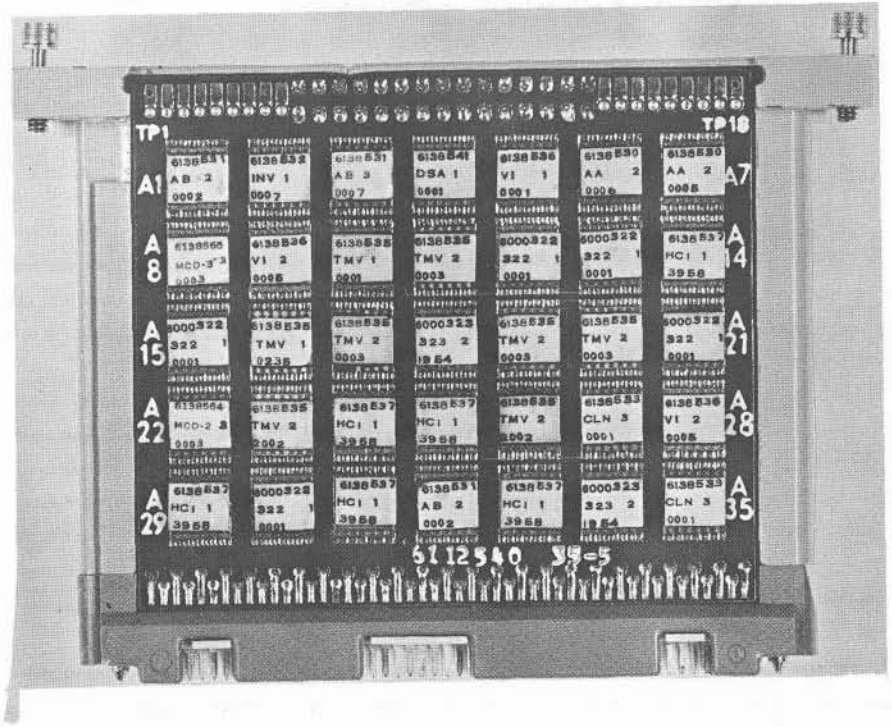

Figure 4.5.1-3. Multilayer Interconnection Board.

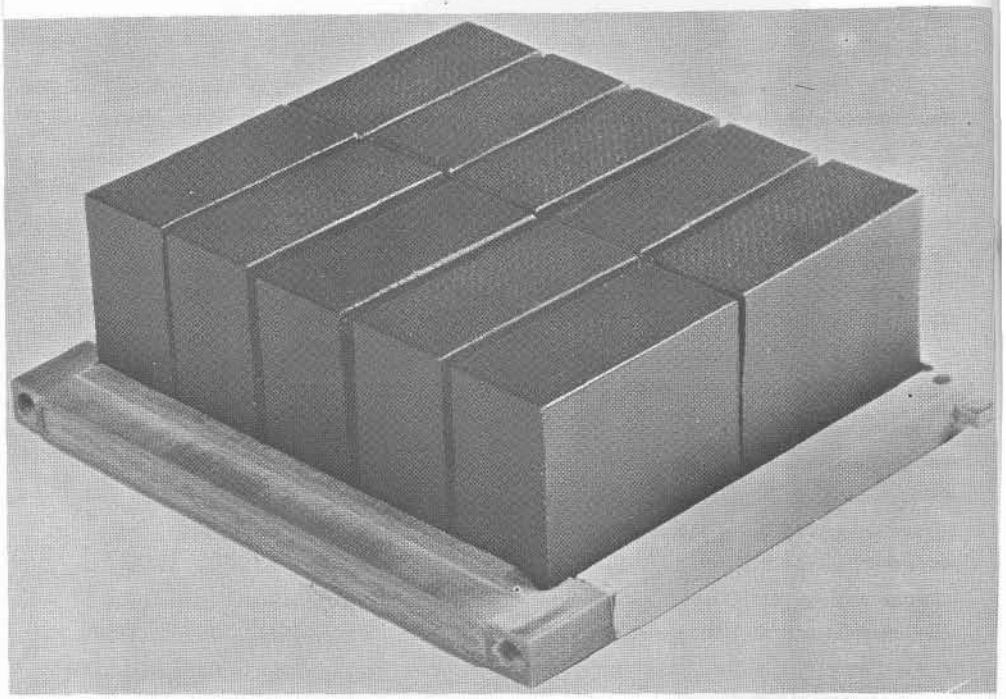

Figure 4.5.1-4. Page Assembly.

mounted on the interconnection boards previously mentioned. In volume, one circuit module page is equivalent to three unit logic device pages. Figure 4.5.1-4 shows a circuit module page assembly..

The magnesium-lithium frames of the digital computer and the data adapter are liquid cooled to remove heat generated by the electronic components. This cooling results in a low operating temperature for the electronic components and thus in a high reliability for the devices.

The use of various redundancy techniques for further improvement of the reliability considerably increases the number of electronic components required in a system. In the case of triple modular redundancy, approximately 3.4 times as many components are required as in a simplex system. However, with the application of redundant logic, several failures are possible without a system failure. Thus, despite the increase of component failures with the number of components, a triple modular redundant system is more reliable than a simplex system by a factor of approximately $(3R-2R^2)^N$, where R is the reliability of a module and N is the number of modules in a simplex machine. To guarantee effective triple modular redundancy before launch, component failures will

be reported by disagreement detectors and the modules concerned will be replaced by the plug-in page assemblies shown in Figures 4.5.1-3 and 4.5.1-4.

The following sections describe the computer and data adapter and show how these units are integrated into the launch vehicle guidance and control system.

4.5.2 General Description of the Launch Vehicle Digital Computer

The digital computer is a serial, fixed-point, stored program, general purpose machine. Special algorithms have been developed and implemented for multiplication and division [19]; multiplication is done four bits at a time and division is done two bits at a time. The machine utilizes random-access magnetic core memory, triple modular redundancy logic for the central computer, and duplex memory modules. Ultrasonic glass delay lines are used as serial arithmetic registers and as dynamic storage for the instruction counter. The delay lines are used similarly to revolvers in a drum machine and provide temporary storage at relatively small weight and volume. Salient characteristics of the computer are summarized in Table 4.5.2-1. Data words of 28 bits (25 magnitude bits, 1 sign bit, and 2 parity bits) are used in computation. The memory is arranged so that one data word or two instructions (each instruction then contains a parity bit) may occupy one 28-bit memory word.

Each memory module consists of fourteen 128 x 64 magnetic core planes plus the required drive and sensing circuits. The basic module contains 4096 nonredundant 28-bit words. For flexibility in memory size, the number of modules may vary from one to eight. With eight memory modules operating in simplex, the computer has a memory capacity of 32,768 words, which is equivalent to the basic memory capability of the IBM 7090 commercial machine. The memory modules operate independently, allowing duplexing for higher reliability. Storage external to the memory is located predominantly in the glass delay lines.

The reliability of the computer is predicated on the use of triple modular redundancy in the central computer logic. Figure 4.5.2-1 indicates the organization of the computer from a reliability standpoint. Calculations and simulations based on Monte Carlo techniques indicate a reliability of .996 for 250 hours (.999966 for a six hour mission) for the computer logic and memory using triple modular redundant and duplex techniques, respectively. For comparison, the equivalent simplex logic has a reliability figure of .955 for 250 hours. Theoretically, the reliability of duplex modules exceeds that of triple redundant modules by a factor $\frac{2R-R^2}{3R^2-2R^3}$, but the difference is of a second order effect for values of R close to "one" and therefore negligible. Duplex redundancy, however, has limited application because of the problem of determining which one of the two units failed.

The triple modular redundant logic system uses three identical simplex logic channels and subdivides each channel into seven functional modules. The outputs from corresponding modules are voted upon in voter circuits before the signal is sent to the next modules. Figure 4.5.2-2 shows

Table 4.5.2-1. Computer Characteristics

Type	Stored program, general purpose, serial, fixed point, binary
Clock	2.048 MHz clock, 4 clocks per bit, 512 kilobits per second
Speed	Add-subtract and multiply-divide, simultaneously
Add Time, Accuracy	82 μs, 26 bit
Multiply Time, Accuracy	328 μs, 24 bit
Mult-Hold Time, Accuracy	410 μs, 24 bit
Divide Time, Accuracy	656 μs, 24 bit
Memory	Random access toroidal core
Storage Capacity	Up to a maximum of 32,768 28-bit words in 4096 word modules
Word Length	Memory word 28 bits: Two instructions may be stored in 1 memory word
Data	26 bits plus 2 parity bits
Instruction	13 bits plus 1 parity bit
Input/Output	External: computer-programed Input/Output Control: external interrupt provided
Component Count*	40,800 silicon semiconductors and cermet resistors Up to 917, 504 toroid cores
Reliability*	0.996 probability of success for 250 hours using TMR logic and duplex memory modules
Packaging	Structure constructed of magnesium-lithium material, designed to house 73 electronic pages and 8 memory modules
Weight* [kg]	30 (4 memory modules)
Volume* [m^3]	0.07
Power* [W]	150.0 (4 memory modules)

*Figures given here are estimated values.

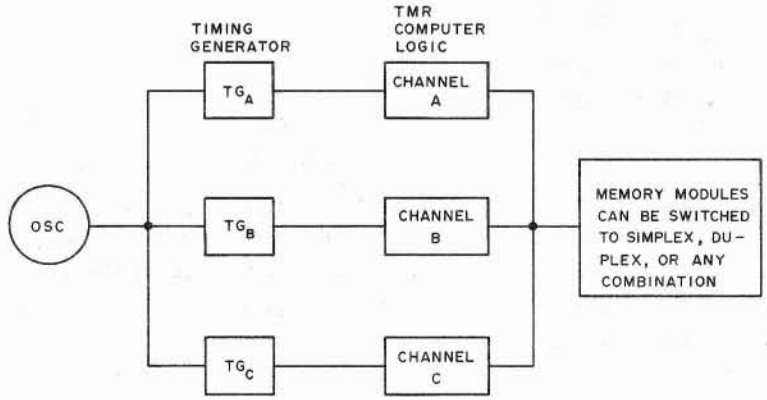

Figure 4.5.2-1. Computer Redundancy Configuration.

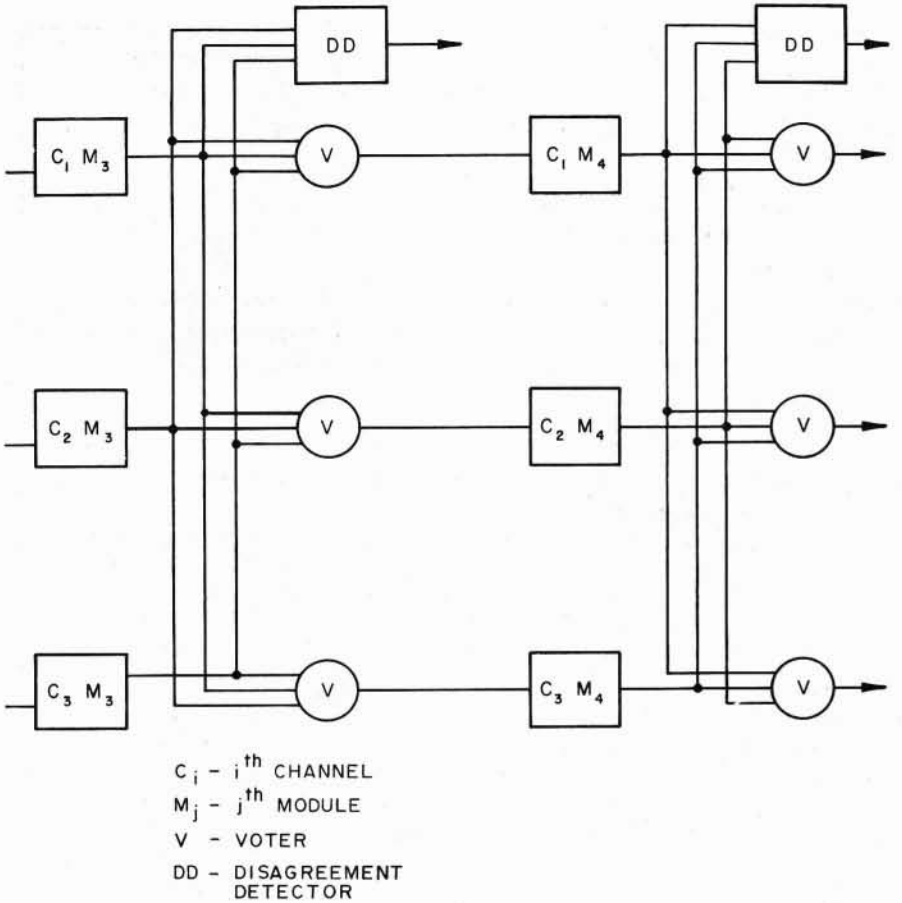

Figure 4.5.2-2. Triple Modular Redundancy.

typical modules and voters. The output of the voter circuit is equal to the majority of the inputs to the circuit. Thus, even if one of the three inputs is incorrect, the output to the next module will be correct. The voter circuit outputs may go to any of the other subdivided modules of the computer. This allows correct computations to be obtained, even with several malfunctions in the computer, provided two modules of a triple redundant set are not in error.

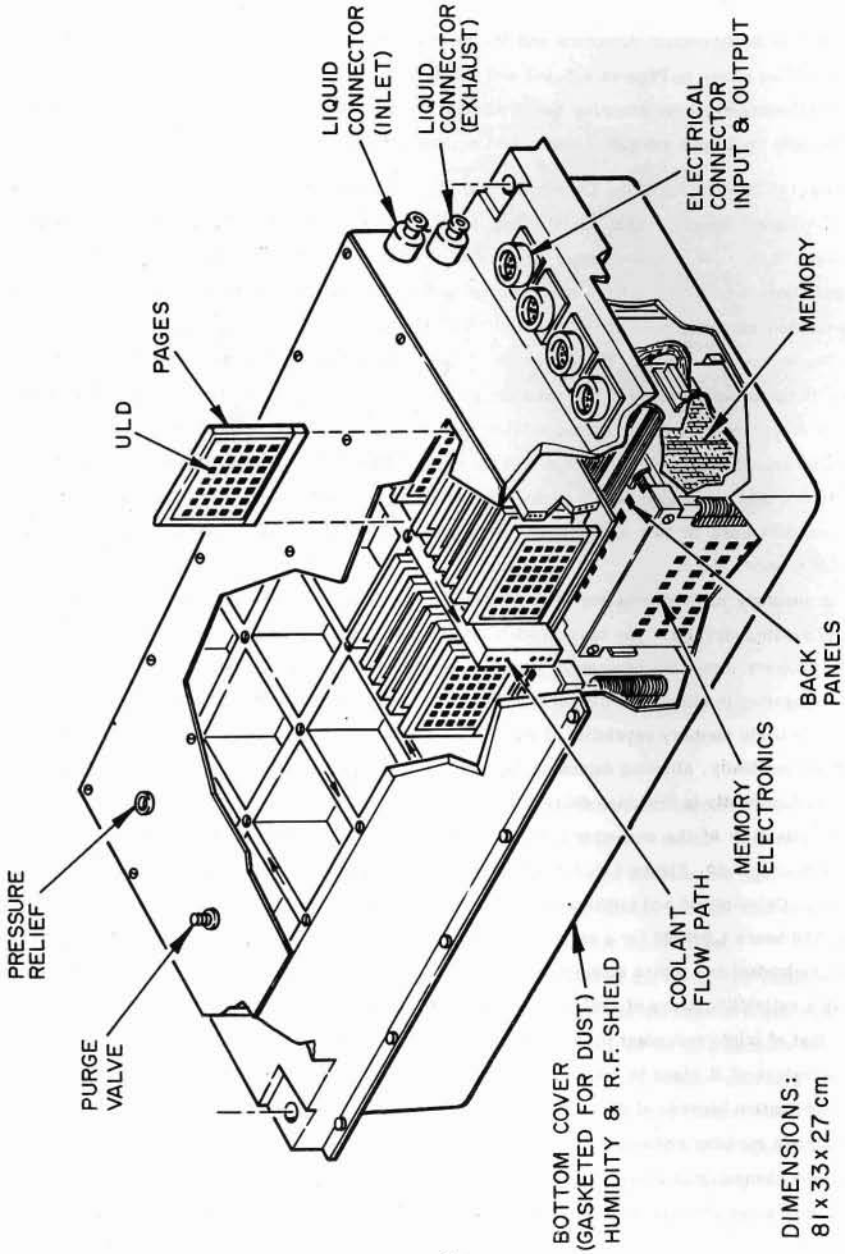

Figure 4.5.2-3. Cutaway View of Digital Computer.

Disagreement detectors are used on module outputs as shown in Figure 4.5.2-2 to indicate a failure in the system. Approximately 13 disagreement detectors are logically combined and fed to a register in the data adapter. These signals are then fed to the telemetry buffer register for monitoring either before launch or in flight.

A cutaway view of the digital computer is given in Figure 4.5.2-3.

4.5.3 General Description of the Launch Vehicle Data Adapter

The launch vehicle data adapter is the input/output unit for the launch vehicle digital computer and communicates with other equipment in the launch vehicle and with the ground checkout equipment. The data adapter is capable of transforming input and output signals acceptable to the digital computer and other interconnected equipment. It controls data flow, provides temporary data storage where necessary, and performs certain simple computational and logical operations on data. The functions and interfaces of the data adapter are shown in block diagram form in Figure 4.5.3-1.

To interface digital and analog equipment, the data adapter is capable of converting signals in either direction as required.

In particular, the data adapter supplies data to and accepts data from the digital computer at a 512 kHz rate upon command by the digital computer. It accepts and decodes data address signals from the digital computer and provides the digital computer with interrupts and miscellaneous control signals. It also accepts synchronizing signals from the digital computer and generates a set of timing signals that is in synchronism with those of the digital computer.

Furthermore, the data adapter provides regulated dc power for its own operation and for the digital computer; it also contains circuitry for channel switching, power supply switching, and sequencing. Data adapter ac power supplies excite the resolvers on the platform with sinusoidal voltage.

A summary of the data adapter characteristics is shown in Table 4.5.3-1.

To improve reliability, various types of redundancy are employed throughout the data adapter. Figure 4.5.3-1 indicates the type of redundancy used in each part. Triple modular redundancy is employed in the flight critical portion of the digital circuitry similar to its application in the digital computer logic.

Power supplies are used in duplex redundancy; isolation diodes allow one amplifier to continue its operation in case of a failure of the other amplifier.

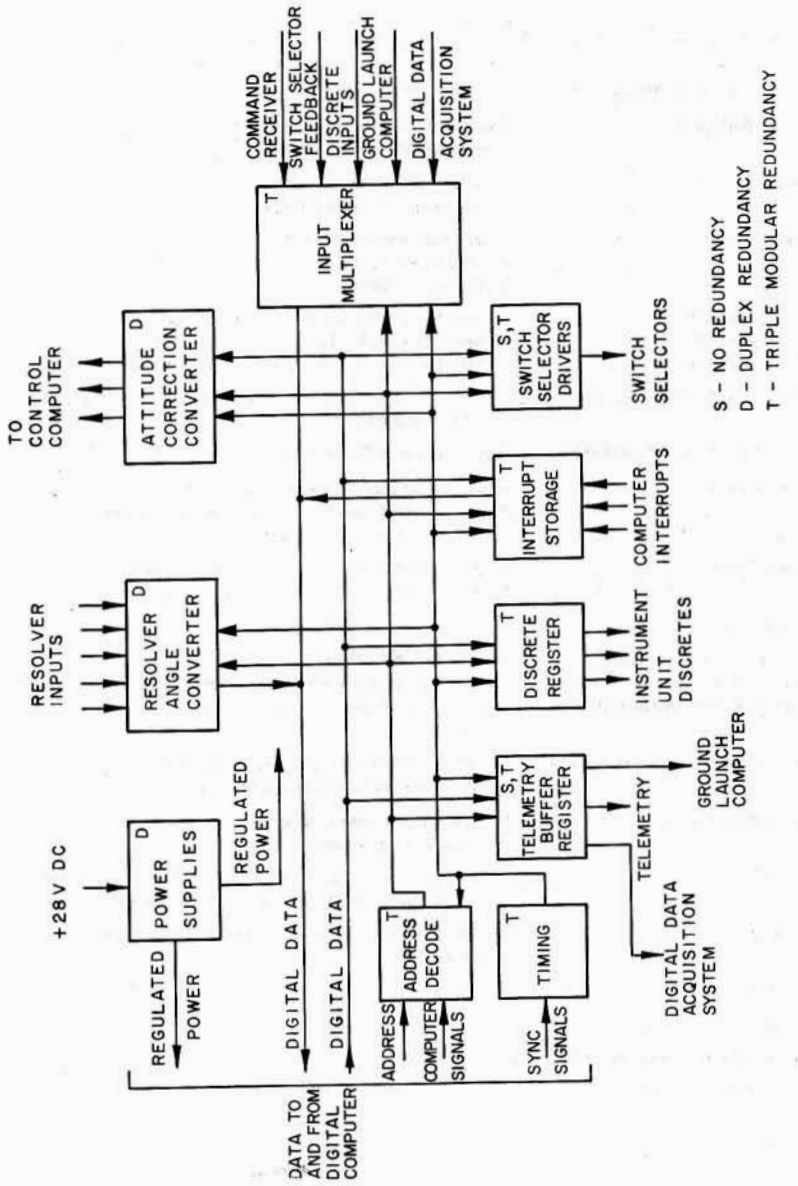

Figure 4.5.3-1. Data Adapter/Computer Interface.

Table 4.5.3-1. Data Adapter Characteristics

ITEM	DESCRIPTION
Computer Input/Output Rate	512-kHz serial
Power Supplies	6 duplexed regulated dc supplies 2 ac resolver power supplies
Switch Selector	8-bit switch-selector input 15-bit switch-selector output
Discretes	7 interrupt inputs from IU 13 discrete outputs 32 discrete inputs
Buffer Register Tag Register Mode Register	26 bits) provides communication with 9 bits) the RCA-110 ground control computer, 6 bits) telemetry transmitter, and DDAS
Digital-to-Analog Converter	8 bits plus sign, 2-millisecond operation, 3 attitude commands, and 2 spare outputs
Analog-to-Digital Converter	Equivalent of 17 bits from a two-speed resolver
Platform	4 two-speed gimbal angle resolver inputs 6 single-speed accelerometer resolver inputs
Spares	4 single-speed resolver inputs
Delay Lines	3 four-channel delay lines for normal operations 1 four-channel delay line for telemetry operations
Telemetry	
Command Receiver	14 bits for input data
Data Transmitter	38 data and identification bits plus validity bit and parity bit
Digital Data Acquisition	15 bits address plus validity bit for output data, 10 bits for input data
Input from RCA-110 Computer	39 data and identification bits plus validity bit for output data 14 bits for input data plus interrupt
Component Count	37,000 silicon semiconductors, cermet resistors, and other special components
Reliability	0.99 probability of success for 250 hours of operation; uses TMR logic, duplex special circuits, duplex power supplies
Packaging	125 electronic page assemblies plus special electronic assemblies
Weight [kg]	80
Volume [m^3]	0.1
Power without Computer [W]	320

4.5.4 Functional Aspects of the Computer System

This section discusses some of the functional aspects of the computer and data adapter and indicates how they are integrated into the overall vehicle system. The cases considered represent only typical functions.

The primary purpose of the computer system is to issue control commands and flight sequence signals to the vehicle system during flight. These signals can be considered dynamic in nature because they result in vehicle motion or action. Other functions can be considered passive, but nevertheless are of extreme importance. They include the operation of the computer system with the telemetry system, the ground launch computer, and the radio command system. The ground launch computer is used during ground checkout, whereas the radio command system and the telemetering system are operational in ground checkout as well as in flight.

The control commands are evaluated in a major and a minor computation cycle. During the major cycle, which occurs approximately once per second, a solution to the guidance equation is obtained. The guidance equation is a function of vehicle position ($\bar{R}$), vehicle velocity ($\dot{\bar{R}}$), acceleration ($\frac{\bar{F}}{m}$), and real time (t). All parameters, with the exception of real time, are derived from the velocity measurement inputs; time is accumulated in the data adapter. Other operations performed during the major loop are vehicle sequencing for flight events, discrete outputs, telemetry outputs, and miscellaneous control functions within the data adapter.

During the minor loop, the vehicle attitude correction is computed. Attitude correction outputs $\Delta\phi_{x,y,z}$, shown in Figure 4.5.4-1, are dependent upon platform gimbal angles $\theta_{x,y,z}$ and upon the result of the guidance equation calculated in the major loop. The minor loop calculations are made approximately 25 times per second. The attitude correction signals must be updated often enough that the frequency of the discrete steps is above any critical frequency caused by sloshing and bending of the vehicle and that the attitude correction change occurring between any two sampling periods is small. These criteria are necessary to prevent the discrete nature of the attitude correction angles from causing any perturbations in the vehicle attitude or causing the vehicle to become unstable.

As indicated in Figure 4.5.4-1, the digital computer is stepped through the computation cycles by a set of instructions stored in the computer memory. If the digital computer is in the major computation loop, it will obtain vehicle velocity information from the optical encoders (optisyns) and accelerometers on the stabilized platform. These optisyns generate electrical square-wave signals (gray code) which indicate the rotations of the accelerometer shafts. These optisyn signals are converted into true binary numbers in the data adapter. The resolution of the converted accelerometer data is 0.05 m/s.

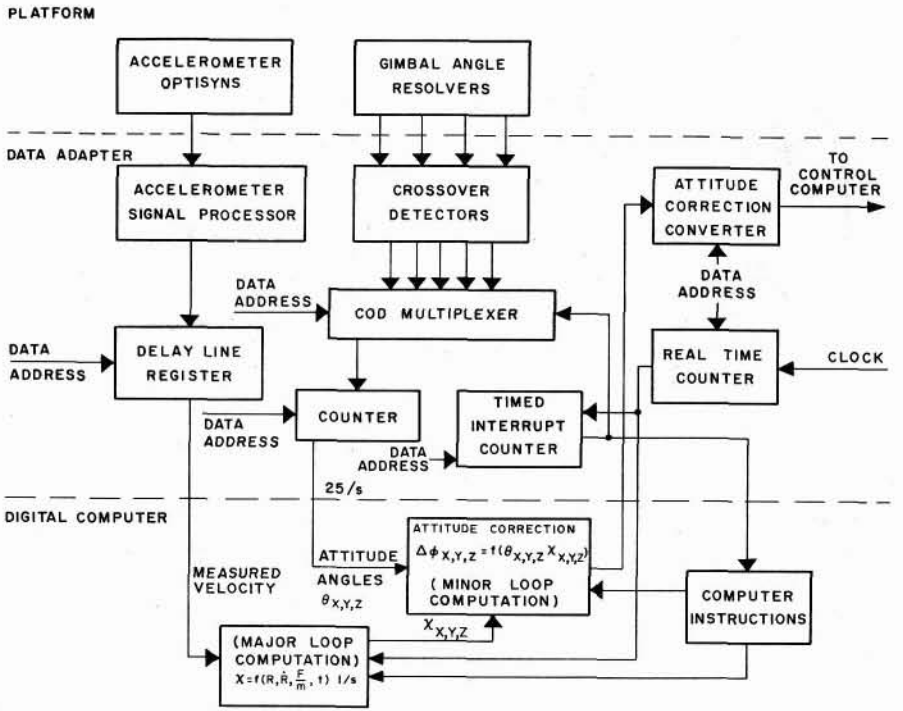

Figure 4.5.4-1. Navigation and Guidance Computations.

The velocity readings from the platform integrating accelerometers are combined with the gravitational acceleration to yield the velocity components $\dot{X}$, $\dot{Y}$, $\dot{Z}$, which are accumulated in the computer. By time integration of the velocity components, the vehicle position R (X, Y, Z) is computed.

To obtain the thrust acceleration $\frac{F}{m}$ required for guidance computations, the velocity readings are differentiated (division of the incremental velocity readings by the time elapsed between two readings). From the resulting acceleration components, the term $\frac{F}{m}$ is computed by taking the square root of the sum of the squares (Fig. 4.5.1-1).

Real time is accumulated in a delay line in the data adapter by counting computer phase times. Whenever the accelerometer optisyns are read, the real time increment in the data adapter is also read. The real time increments are combined in the digital computer with the old values to produce the new values of real time that existed when the accelerometers were read.

The discussed values such as real time, absolute acceleration, vehicle position, and vehicle velocity are used during the major loop computation to calculate the desired gimbal or χ angles. These χ angles are used during the minor loop computations.

During the major computation loop, the digital computer also selects and reads the coarse gimbal angle resolvers located on the stabilized platform. The resolver signals are selected and gated through the multiplexer by energizing a set of data address lines with a digital address.

The computer program enters the minor loop by a signal from the minor loop timed-interrupt counter. The computer stores in the counter a number that is counted down to zero. When it reaches zero, a signal is sent to the digital computer that causes it to switch from major loop computations to minor loop computations.

The signal also selects the first fine gimbal angle resolver and gates the resolver signal through the multiplexer to the counter. By the time the computer processes the interrupt and switches to the minor loop, the first gimbal angle reading is in the counter and is ready for use by the computer. The computer data address that gates the counter reading into the computer also gates the next fine gimbal angle resolver signal through the multiplexer to the counter.

The fine gimbal angle readings are combined in the computer to form the total gimbal angle. This value is compared to the coarse gimbal angle readings as a check against failures. The gimbal angles ($\theta_{x,y,z}$) and the extrapolated values of the χ angles ($\chi_{x,y,z}$) are used in the minor computation loop to obtain attitude correction angles.

After the attitude correction angles are computed, they are sent to the attitude correction converter in the data adapter, converted to analog signals, and routed to the proper output channel by data address signals from the digital computer.

As previously stated, the rate at which the attitude correction signals are updated is an important factor for vehicle stability. The attitude error angles are updated 25 times per second or every 40 ms. The minor loop program requires approximately 18 ms to read all the fine gimbal angles and compute the attitude correction angles.

After the three attitude-correction angles have been sent to the data adapter, the digital computer enters a number into the minor loop timed-interrupt counter. This number represents the time-to-go to the beginning of the next minor computation loop. After this operation, the computer program returns to the point from which it left the major loop and continues major loop computation until another minor loop interrupt is generated by the minor loop timed-interrupt counter.

4.6 Control Computer and Control Sensors [20]

4.6.1 Control Computer

During powered flight, the incoming analog signals are filtered and summed with the proper polarity and relative gain factors in the control computer to form individual commands for each

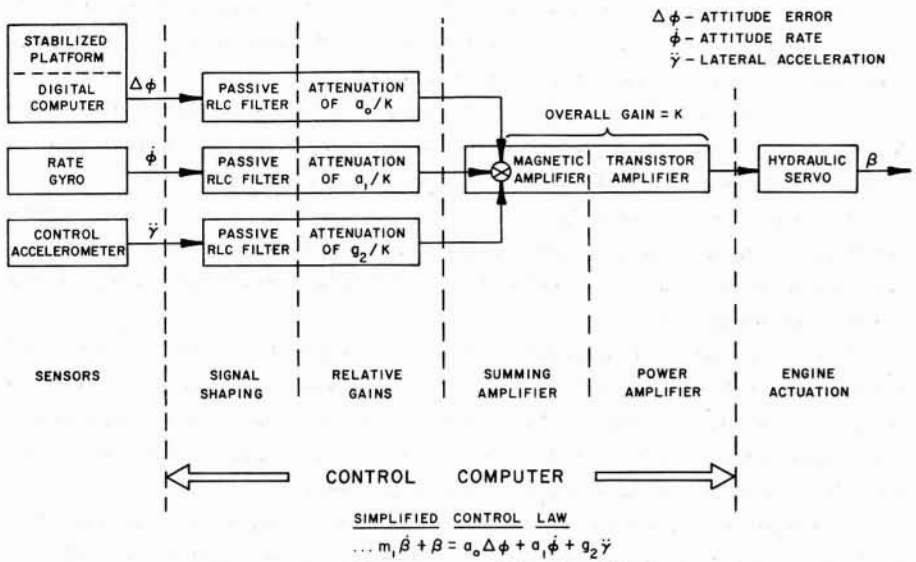

Figure 4.6.1-1. Elements of the Control Computer.

hydraulic servoactuator of the engine gimbaling system. Figure 4.6.1-1 shows a diagram of the major elements of the control computer required to form the command of one axis only for one engine servo. Figure 4.6.1-2 shows a functional sketch of the actuator orientations on the different stages. Simultaneous equal commands to the pitch or yaw servos result in net thrust deflections in the pitch or yaw plane. For the first and second stages, roll torques are initiated by simultaneous commands to the pitch and yaw servos. Roll torques are produced from the auxiliary propulsion system during the third stage of flight.

The signal shaping or filtering of information obtained from the stable platform, rate gyros, and body-fixed control accelerometers is performed by passive RLC networks. The primary purpose of these shaping circuits is to stabilize the vehicle structural bending either by attenuating the signals of frequencies near the bending modes or by phase shifting them. A typical filter that might be used to compensate the output of a rate gyro is shown in Figure 4.6.1-3. From the Bode plot, it is apparent that the filter will have very little effect in the frequency range of the dominant control mode; however, it supplies sufficient phase lag to stabilize the first bending mode and sufficient attenuation to stabilize all higher bending modes. The filters that are typically used to compensate the attitude error signals and body-fixed accelerometer signals are less complicated since bending pickup of the stabilized platform is less severe and the band-pass requirement on the accelerometer control loop is small.

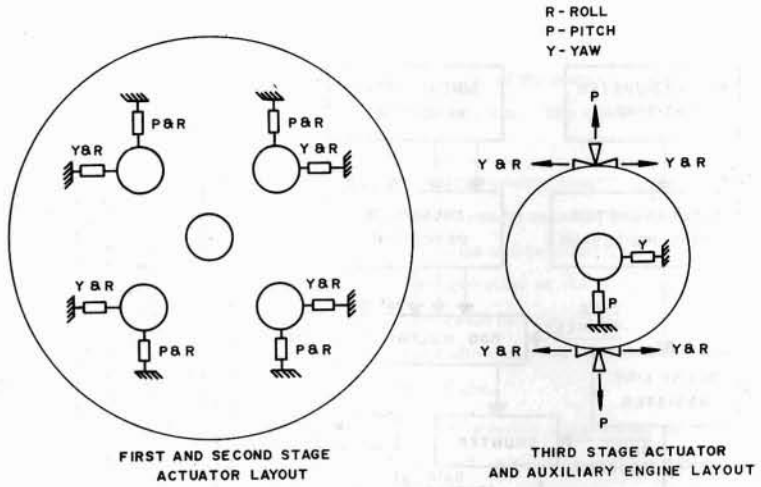

Figure 4.6.1-2. Arrangement of Actuators.

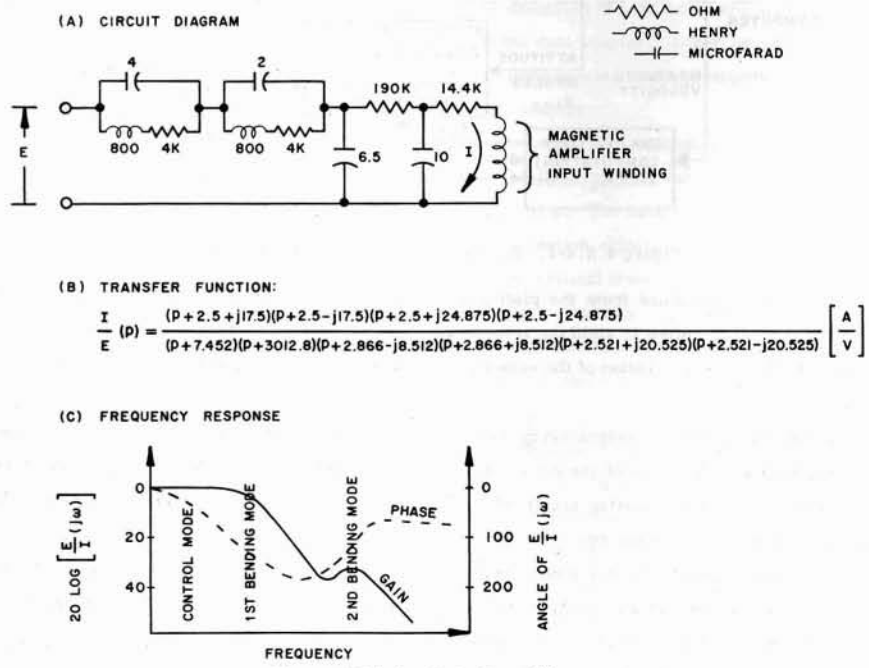

Figure 4.6.1-3. Rate Gyro Filter.

The modified pitch and yaw input signals are superimposed on the corresponding roll signals as required for individual actuator control by magnetic amplifiers. Since the magnetic amplifiers are current summing devices, the attenuation circuits are simply series resistance. To provide gain factor adaptation, provisions are made for changing this resistance discretely or continuously as a function of flight time. The continuous resistance programing with time is accomplished by a synchronous motor driving a potentiometer through a cam mechanism.

After the signals have been processed in the magnetic amplifiers, transistorized power output stages provide direct current drive to the engine position servos of the first stage; after separation, switchover to the second stage servos occurs. The third stage of the Saturn V has only one control engine and therefore two position servos. Thus six of the servoamplifiers are available to provide a triple redundant driving circuit for each servo.

During coasting periods, the torques needed for attitude control are supplied by an auxiliary propulsion system composed of six small hypergolic rocket engines oriented as shown in Figure 4.6.1-2. The control computer supplies individual firing commands to each of these engines based on a switching scheme designed to minimize fuel consumption. Provisions are made for automatic control or manual control from the Apollo spacecraft. The nonlinear switching characteristics consist of a first order lag circuit in a negative feedback loop around an electronic relay which has variable deadband and hysteresis. All components of the control computer are triple redundant.

4.6.2 Rate Gyros

Vehicle angular rates are obtained by use of rate gyros to provide the damping necessary for stabilizing the vehicle control system. Rate information is often achieved by electrically differentiating the analog attitude signal; however, the digital nature of the Saturn attitude reference system does not readily permit electrical differentiation. Also, rate information obtained from a location different from the attitude sensing location may be required to adequately stabilize the vehicle elastic modes.

Two features have been added to the conventional fluid-damped rate gyro for preflight testing. The first is a torquer about the output axis to produce a signal from the microsyn sensor. Excitation of the torquer stimulates signals from the rate gyro output to the control system. The second feature is a gyro speed indicator, consisting of four small permanent magnet slugs symmetrically spaced around the spin motor wheel; the frequency of the voltage induced in a coil located in the gyro housing is a measure of the gyro motor speed.

A triple redundant arrangement with three rate gyros for each of the three vehicle axes has been selected for angular rate measurements in the IU during orbital and injection phases in contrast to the nonredundant rate gyros in the short-life stages.

4.6.3 Control Accelerometer

The control accelerometer consists of a spring supported mass constrained to move linearily along one axis and is designed to have approximately ±0.1 mm travel for the total acceleration range. The motion of the spring-mass system is fluid damped. Inductive pickoffs are mounted symmetrically and sense the displacement of the spring-mass system. The two inductive elements constitute one half of a bridge type detector. The secondary windings of a 400 Hz transformer complete the bridge detector circuit, whose output is demodulated and amplified.

The accelerometer also contains an internal bidirectional electromagnetic coil that, when excited, produces a force on the accelerometer mass along the input axis. Thus an acceleration can be simulated for testing proper accelerometer operation up until a few seconds before actual flight. The force coil also provides the input for operating the accelerometer in closed loop guidance and control simulation tests.

4.7 Thrust-Vector-Control Servoactuators [21]

The angular direction of the thrust vector of high thrust engines (over 0.5×10^6 N) is best controlled by swiveling the gimbal-mounted propulsion engines. This control is obtained by linear hydraulic servoactuators in the pitch and yaw planes.

The actual arrangement of the actuators for the multiengine first and second stages and the single engine stage of the Saturn launch vehicle is shown in Figure 4.7-1.

During operation of the rocket engine, the hydraulic power supply is usually provided by a hydraulic pump driven by the engine turbine and an accumulator-reservoir to cover peak loads. An auxiliary pump, driven by an electric motor, provides hydraulic pressure for static checkout of the hydraulic system.

This conventional scheme has been applied for the second and third stage control engines; the hydraulic pressure has also been selected conventionally to 2500 N cm^{-2}. For the first stage engines, the hydraulic pressure is received directly from the fuel turbopump at 1400 N cm^{-2}; the fuel is used as hydraulic fluid. The available low operating pressure requires a large servovalve and actuator piston area; however, the pressurization system is very simple and even the accumulator-reservoir can be omitted as a result of the almost unlimited availability of pressurized fuel.

The servoactuators for the Saturn stages have been designed with mechanical feedback to replace the conventional electrical feedback to the driving amplifier located in the control computer. The hydraulic valves employ negative feedback of the actuator piston pressure to reduce actuator resonance resulting from structural compliance and fluid compressibility.

SIMPLIFIED SYSTEM BLOCK DIAGRAM

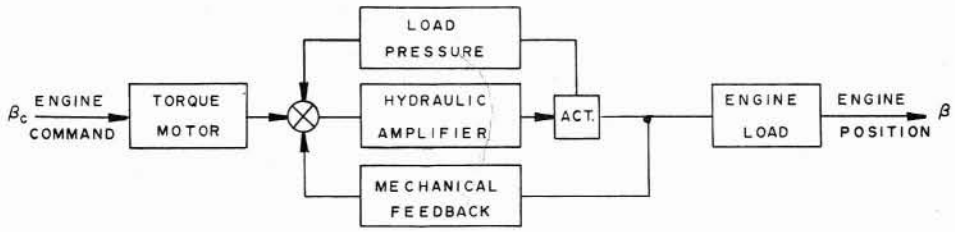

SIMPLIFIED SYSTEM SCHEMATIC

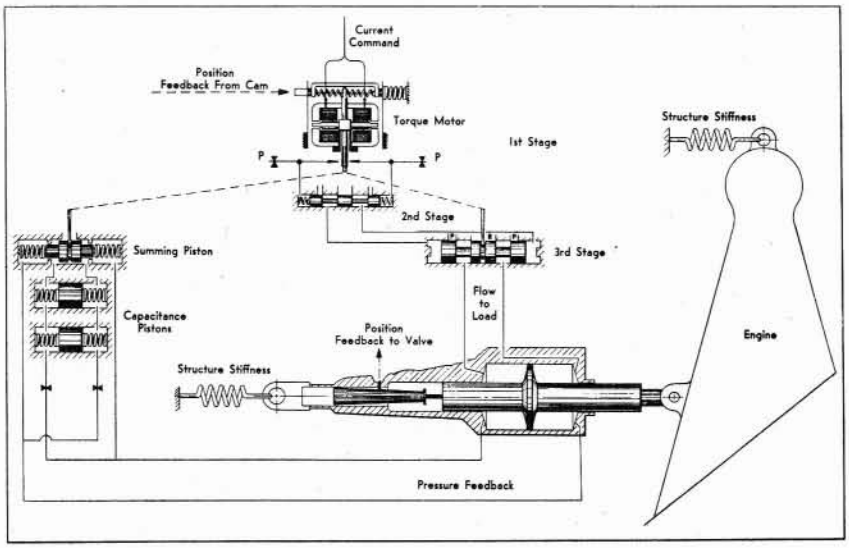

APPROXIMATE LOW FREQUENCY TRANSFER FUNCTION

$$\frac{\beta}{\beta_c} = \frac{1}{m_2 p^2 + m_1 p + 1}$$

STAGE	m_1	m_2
1	0.047	0.0011
2	0.030	0.0011
3	0.049	0.0017

Figure 4.7-1. Hydraulic Actuator System.

5. SUMMARY

5.1 Flight Results

The path adaptive PGM guidance scheme and the guidance and control system have been flight tested on Saturn I vehicles SA-6 and SA-7 with excellent results. The mission of these two vehicles was to inject the payloads into near circular earth orbits. The PGM scheme was employed for guidance in the flight plane, and delta-minimum guidance was employed in the cross range direction. Delta-minimum guidance constrains the vehicle to a reference flight path. The PGM guidance polynomial for SA-7 consisted of 33 terms involving position, velocity, and acceleration; engine cutoff was initiated when the velocity of the vehicle attained a preset value.

The PGM scheme for SA-6 and SA-7 performed as expected. Figure 5.1-1 compares the predicted or nominal values of altitude versus flight time for SA-6 and SA-7 with actual values obtained from tracking information. The deviations from the predicted or nominal values shown in the figures include the effects of hardware tolerances, performance variations, and external perturbing forces. On the SA-6 vehicle, one engine of the first stage failed and was automatically cut off around the 116th second of flight time. This perturbation was corrected by the guidance scheme as can be seen in Figure 5.1-1. The orbital insertion accuracy achieved was well within the prescribed tolerances.

The Saturn I SA-9 vehicle employed the IGM scheme for pitch plane guidance; delta-minimum guidance was used again in the cross range direction. Guidance became active approximately 20 seconds after second stage ignition. The payload was injected into an elliptical orbit having a perigee of approximately 500 km and an apogee of approximately 750 km. Figure 5.1-2 compares the predicted or nominal values of altitude versus flight time with the corresponding values obtained from tracking data. The cross range velocity versus flight time is given in Figure 5.1-3. The deviations from the nominal values shown in the graphs include the effects of hardware tolerances, performance variations, and external perturbing forces. The guidance accuracy and performance achieved with the IGM scheme on the SA-9 vehicle was excellent. Moreover, preflight experience with this scheme substantiates its expected flexibility to mission and vehicle changes.

A comparison of the altitude profiles given in Figures 5.1-1 and 5.1-2 shows a considerable difference. The SA-6 and SA-7 vehicles ascended above the desired cutoff altitude and then descended to the desired injection point. This trajectory shape is a feature of optimized trajectories for high performance vehicles, i.e., for vehicles with high thrust-to-weight ratios. The maximum altitude of the trajectory depends on the vehicle performance and the specified end conditions. The SA-7 vehicle reached a higher altitude than the SA-6 vehicle, which had a lower performance because of the engine-out condition. The SA-9 vehicle approached the desired cutoff altitude from below. It had just enough performance to fulfill the required end conditions.

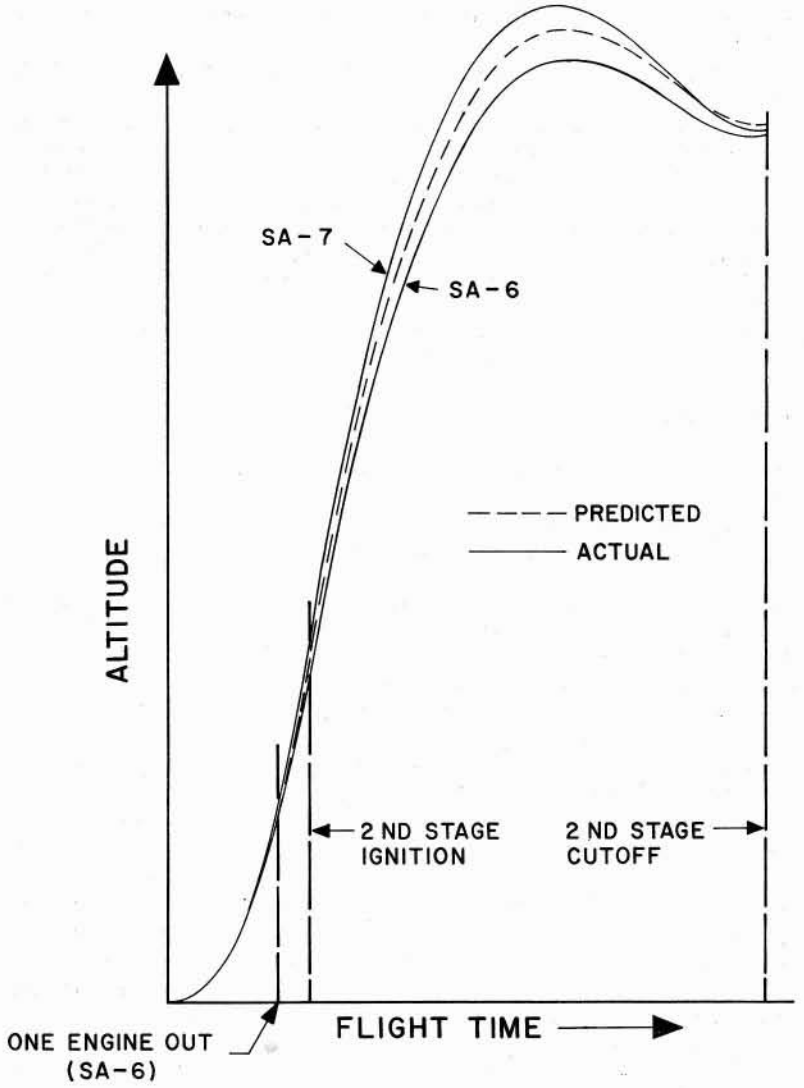

Figure 5.1-1. Predicted and Actual Altitude Versus Flight Time for the SA-6 and SA-7 Vehicles.

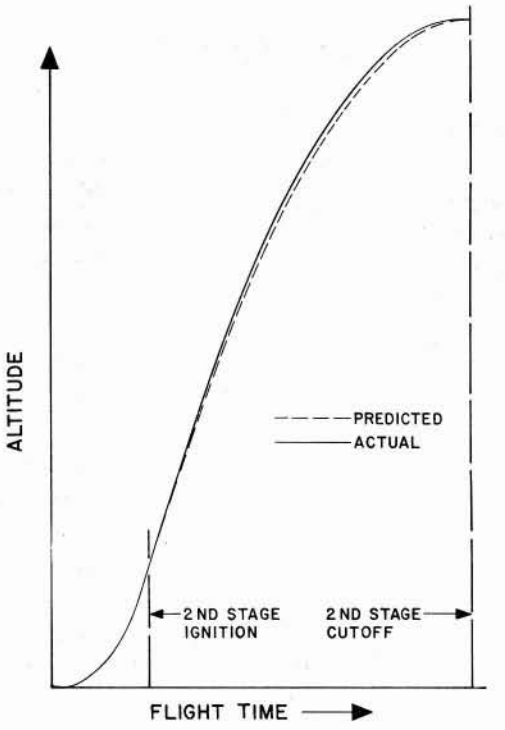

Figure 5.1-2. Predicted and Actual Altitude Versus Flight Time for the SA-9 Vehicle.

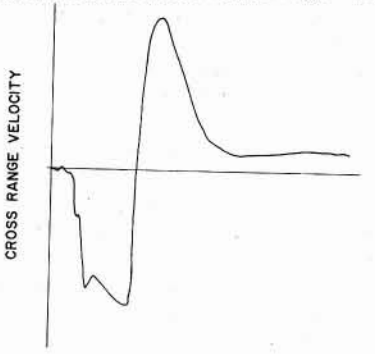

Figure 5.1-3. Actual Cross Range Velocity Versus Flight Time for the SA-9 Vehicle.

CONVERSION TABLE

670 N - 150 lb	.0015 cm - .0006 in.
102×10^3 N - 23,000 lb	.002 cm - .0008 in.
0.9×10^6 N - 200,000 lb	1.44 cm kg (torque) - .104 ft lb
4.5×10^6 N - 1,010,000 lb	900 g - 1.98 lb
6.7×10^6 N - 1,500,000 lb	300 ms^{-1} rev^{-1} - 984 ft/sec/rev
33.5×10^6 N - 7,500,000 lb	0.05 ms^{-1}/bit - .19 in./sec/bit
34×10^6 N - 7,600,000 lb	7.5 mm - .29 in.
12 km (altitude) - 39,000 ft	30 kg - 66 lb
5000 kg - 11,000 lb	.07 m^3 - 2.5 ft^3
2500 kg - 5,500 lb	80 kg - 176 lb
1000 kg - 2,200 lb	0.1 m^3 - 3.5 ft^3
1100 kg - 2,400 lb	0.05 m/s - .2 in./sec
5 kg - 11 lb	0.1 mm - .004 in.
Hz - cps	0.5×10^6 N - 110,000 lb
10 N cm^{-2} - 14.5 psi	2500 N cm^{-2} - 3625 lb/$in.^2$
2000 cm^3/min - 122 $in.^3$/min	500 km - 310 mi.
2400 cm^3/min - 146 $in.^3$/min	750 km - 466 mi.

REFERENCES

1. Haeussermann, W., F. B. Moore, and G. G. Gassaway: Guidance and Control Systems for Space Carrier Vehicles, Astronautical Engineering and Science, pp. 160-177, McGraw-Hill Book Company, Inc., 1963.
2. Hoelker, R. F. and W. E. Miner: Introduction to Concept of the Adaptive Guidance Mode, Aeroballistics Internal Note 21-60, Marshall Space Flight Center, Huntsville, Alabama, December 28, 1960.
3. Geissler, Ernst D., and W. Haeussermann: Saturn Guidance and Control, Astronautics, Vol. 7, No. 2, February 1962.
4. Schmieder, D. H., and N. J. Braud: Implementation of the Path Adaptive Guidance Mode in Steering Techniques for Saturn Multistage Vehicles, American Rocket Society Reprint 1945-1964, August 1961.
5. Smith, I. E., J. J. Hart, and Doris C. Chandler: Procedure for Implementing a Simplified Path Adaptive Guidance Scheme, Aeroballistics Internal Note 25-62, Marshall Space Flight Center, Huntsville, Alabama, February 6, 1963.
6. Chandler, Doris C., H. J. Horn, and Daniel T. Martin: An Iterative Guidance Scheme and Its Application to Lunar Landing, MTP-AERO-63-44, Marshall Space Flight Center, Huntsville, Alabama, February 6, 1963.
7. Smith, I. E., and E. T. Deaton, Jr.: An Iterative Guidance Scheme for Ascent to Orbit (Sub-orbital Start of the Third Stage), MTP-AERO-63-44, Marshall Space Flight Center, Huntsville, Alabama, May 29, 1963.

8. Horn, H. J.: Application of an "Iterative Guidance Mode" to a Lunar Landing, presented at the Third European Space Flight Symposium, 15th Annual Meeting of the DGRR, Stuttgart, Germany, May 22-24, 1963.
9. Space Technology, Edited by Howard S. Seifert, John Wiley and Sons, Inc., New York, N. Y., 1959.
10. Cooper, F. Don: Implementation of the Saturn V Guidance Equations for Lunar Missions from an Earth Parking Orbit, presented at the 12th Flight Mechanics, Dynamics, Guidance and Control Panel Meeting, Manned Spacecraft Center, Houston, Texas, April 13-14, 1965.
11. Haeussermann, W., and R. C. Duncan: Status of Guidance and Control Methods, Instrumentation, and Techniques as Applied in the Apollo Project, presented at the Lecture Series on Orbit Optimization and Advanced Guidance Instrumentation, Advisory Group for Aeronautical Research and Development, North Atlantic Treaty Organization, Duesseldorf, Germany, October 21-22, 1964.
12. Hoelker, R. F.: Theory of Artificial Stabilization of Missiles and Space Vehicles with Exposition of Four Control Principles, NASA Technical Note D-555, National Aeronautics and Space Administration, Washington, D. C.
13. Haeussermann, W.: Stability Areas of Missile Control Systems, Jet Propulsion, ARS, Vol. 27, p. 787, July 1957.
14. Hood, B. N.: S-IC/S-II Separation Control Summary Report, S&ID, North American Aviation, Inc., Downey, California.
15. TRW Space Technology Laboratories: Final Report on Saturn V Control System Studies, Contract NAS 8-2625, Redondo Beach, California, February 28, 1964.
16. The Bendix Corp.: A Description of the ST124-M Inertial Stabilized Platform and Its Application to the Saturn Launch Vehicle, Eclipse-Pioneer Division, Teterboro, N. J., May 1964. Presented at the German Rocket Society Symposium, Darmstadt, Germany, June 26, 1964.
17. Haeussermann, W.: Inertial Instruments with Gas Bearings, Kreiselprobleme Gyrodynamics, IUTAM, Symposium Celerina, Springer-Verlag, Berlin, 1962 (Edited by Hans Ziegler).
18. Bodie, W. G.: Techniques of Implementing Launch Automation Programs (Saturn IB Space Vehicle System), to be presented at the 4th Annual Reliability and Maintainability Conference, Los Angeles, California, July 28-30, 1965.
19. Booth, A. D., and K. H. V. Booth: Automatic Digital Calculators, Academic Press, Inc., New York, N. Y., 1956.
20. Thompson, Z., and R. J. Alcott: Apollo Booster Flight Control System Integration, presented at the SAE A-18 Committee Meeting, Houston, Texas, December 11-13, 1963.
21. Kalange, M. A., and V. R. Neiland: Saturn I Engine Gimbal and Thrust Vector Control System, presented at the National Conference on Industrial Hydraulics, October 17-18, 1963.
22. Smith, Isaac E.: A Three Dimensional Ascending Iterative Guidance Mode, NASA TM X-53258, Marshall Space Flight Center, Huntsville, Alabama, May 12, 1965.
23. Cooper, F. Don: Implementing a Continuous Launch Capability for Saturn V Lunar Missions from an Earth Parking Orbit, NASA TM X-53268, Marshall Space Flight Center, Huntsville, Alabama, May 25, 1965.